



Semi-visible dark photons at the NA64 experiment

13th workshop of the LLP community

Martina Mongillo

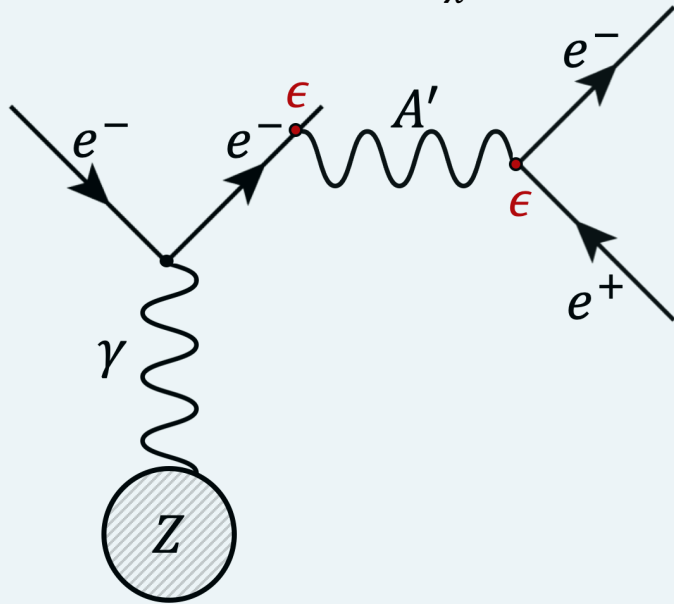
21.06.2023

MINIMAL DARK PHOTON MODELS

Two main scenarios

Visible decay mode

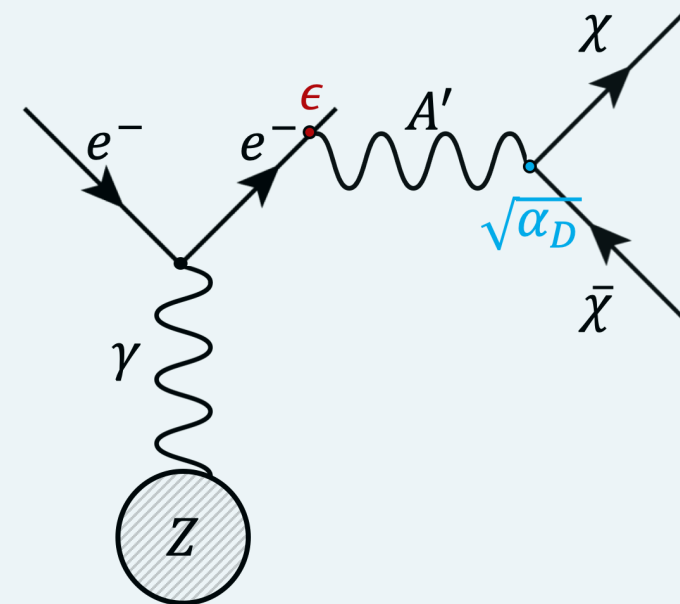
$$(m_{A'} < 2m_\chi)$$



Signature: SM particle pair production

Invisible decay mode

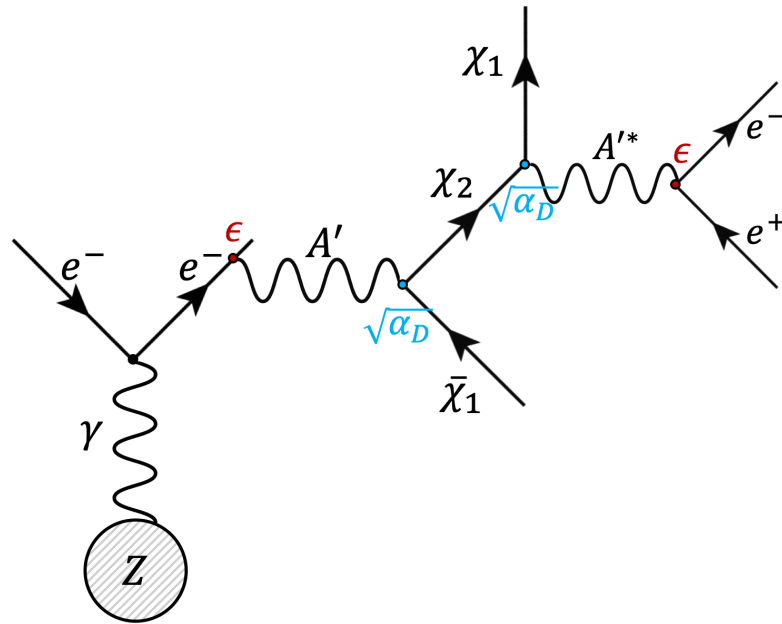
$$(m_{A'} > 2m_\chi)$$



Signature: Missing energy

NEXT-TO-MINIMAL MODELS: SEMI-VISIBLE DECAY

- DS populated by two fermions χ_1 and χ_2 with $\Delta_{21} = m_{\chi_2} - m_{\chi_1} > 0$
- For $m_{A'} > m_{\chi_1} + m_{\chi_2}$ and $\Delta_{21} > 2m_e \rightarrow$ semi-visible cascade $A' \rightarrow \chi_1(\chi_2 \rightarrow \chi_1 e^+ e^-)$



Signature: SM pair production + missing energy

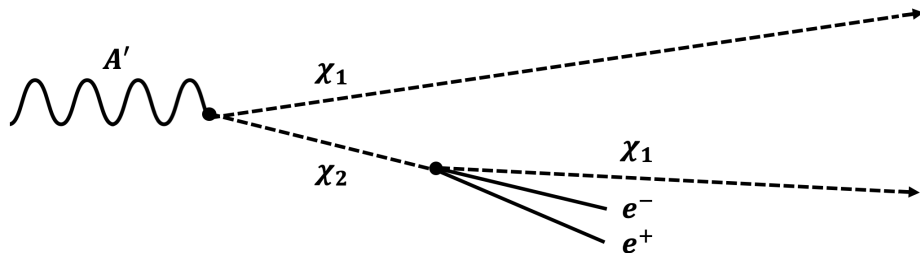
- Visible + invisible final states \rightarrow **semi-visible A'**
- Semi-visible dark photon **can evade traditional bounds** \rightarrow new target for experimental searches

NEXT-TO-MINIMAL MODELS: SEMI-VISIBLE DECAY

Inelastic Dark Matter (iDM)

Izaguirre et al.
PRD 96, 055007 (2017)
Mohlabeng
PRD 99, 115001 (2019)
Duerr et al.
JHEP 02 039 (2020)

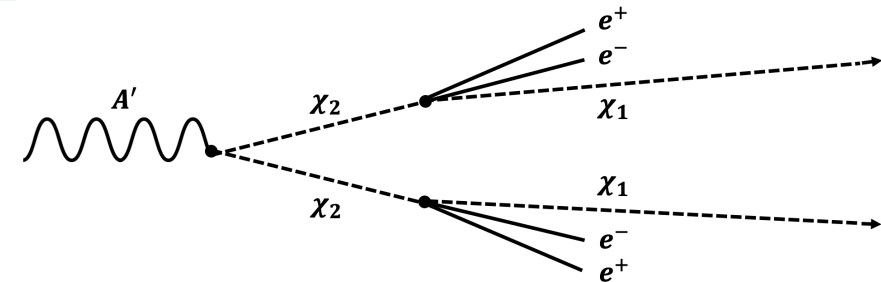
- χ_1 and χ_2 form a **pseudo-Dirac** pair
- Only **off-diagonal** couplings to A' :
 $A' \rightarrow \chi_1 \chi_2$
- Freeze-out through **co-annihilation**
 $\chi_1 \chi_2 \rightarrow A'^* \rightarrow f^+ f^-$
→ no CMB bounds



Inelastic Dirac Dark Matter (i2DM)

Filimonova et al.
JHEP 06, 048 (2022)
Abdullahi et al.
arXiv:2302.05410

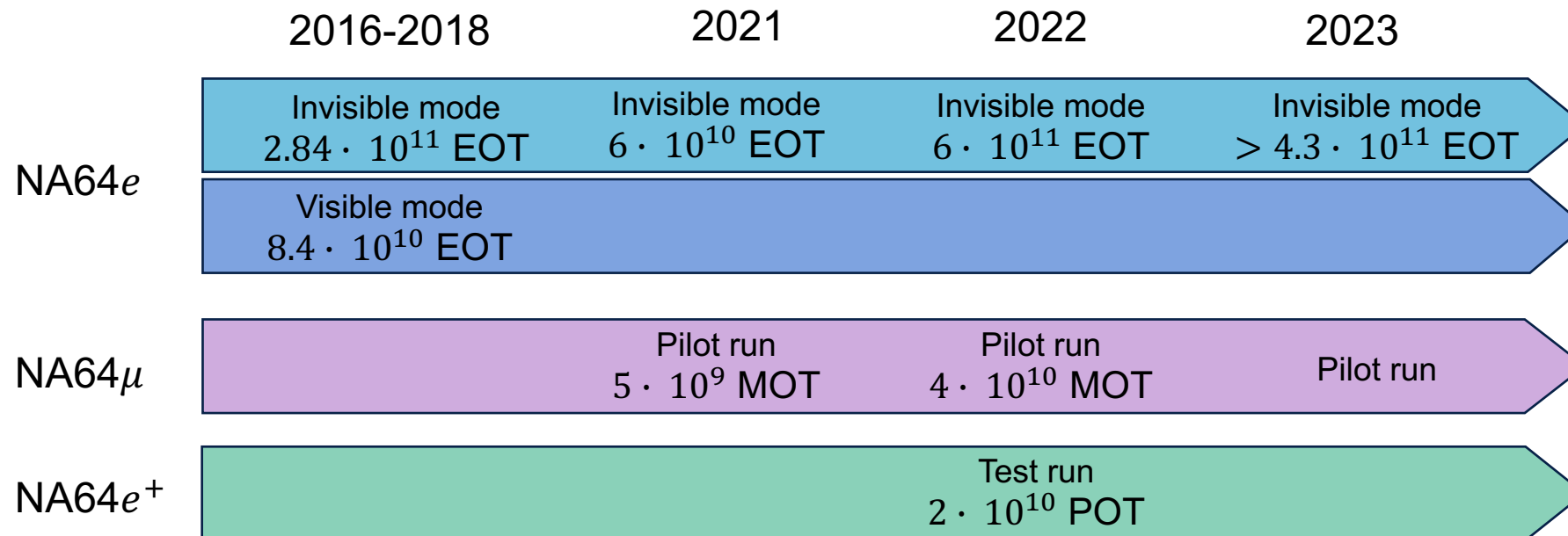
- χ_1 and χ_2 are **exact Dirac** fermions
- Both **diagonal** and **off-diagonal** interactions:
 $A' \rightarrow \chi_i \chi_j, i, j \in \{1, 2\}$
→ Mixing angle θ determines couplings
- Freeze-out through **co-annihilation, co-scattering** and **self-annihilation**
→ Small θ weakens CMB bounds



THE NA64 EXPERIMENT

- **Fixed-target** experiment at CERN SPS (intensity frontier)
- High-purity **100 GeV e⁻** beam (H4 beamline)
- Explores **Dark Sectors in the MeV-GeV** scale
- **Active beam-dump** technique + **missing energy** search
→ signal detection relies only on A' production $\propto \epsilon^2$

- New physics focus:
 - Light dark matter
 - $(g - 2)_\mu$
 - Be anomaly
 - ALPs
 - Z' associated to B-L
 - Z' associated to $L_\mu - L_\tau$

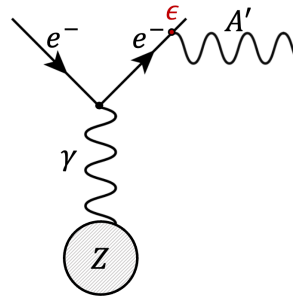


THE NA64 TECHNIQUE

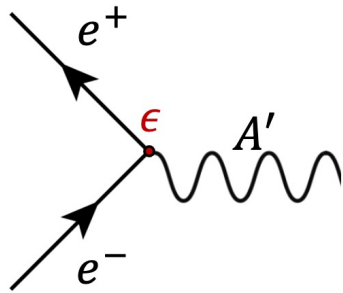
ACTIVE DUMP

Production

- A' -bremsstrahlung



- A' resonant annihilation



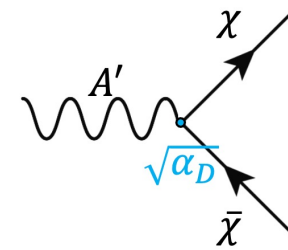
Well-defined beam



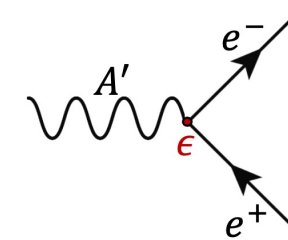
FULLY HERMETIC DETECTOR

Decay

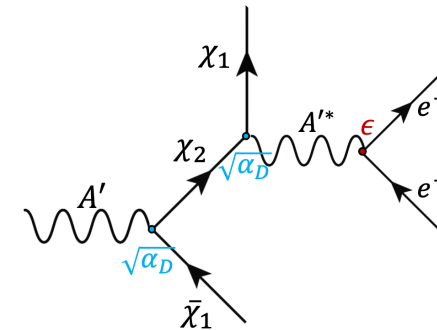
- Invisible
 $m_{A'} > 2m_\chi$



- Visible
 $m_{A'} < 2m_\chi$



- Semi-visible
 $m_{A'} > m_{\chi_1} + m_{\chi_2}$
 $\Delta_{21} > 2m_e$



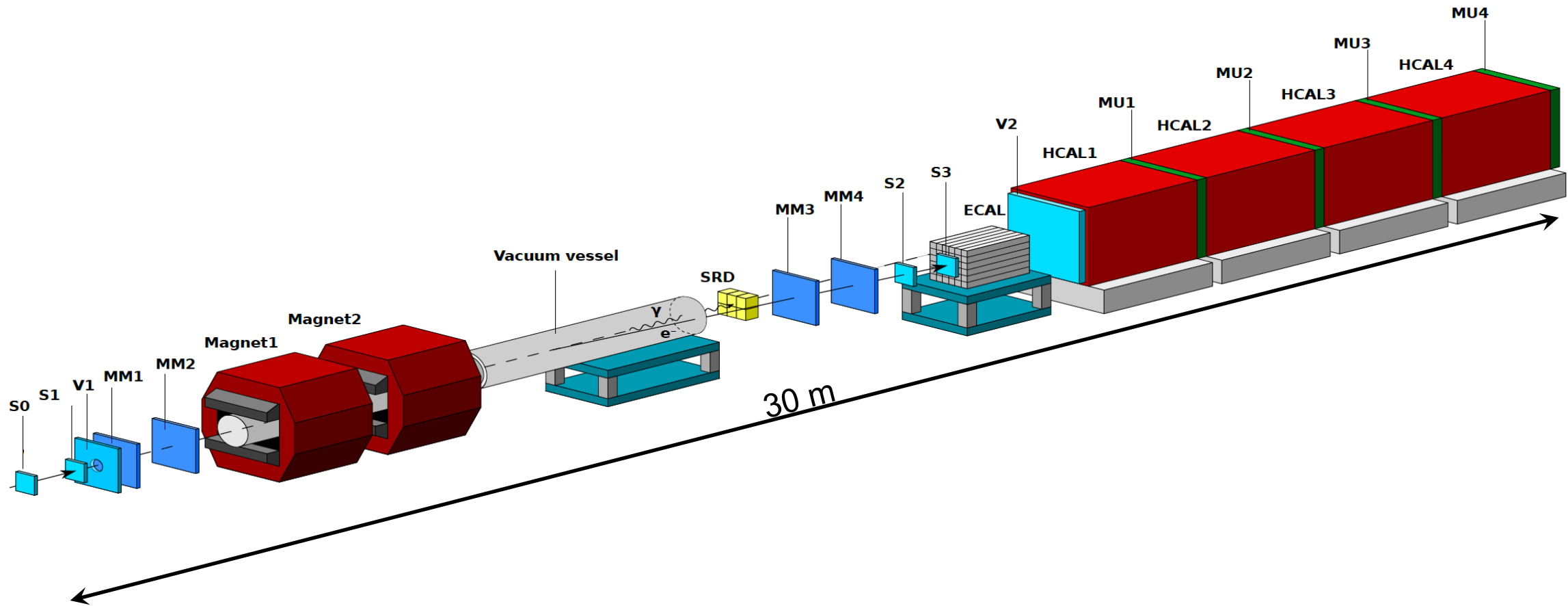
Signature

Missing energy

SM particle pair

Missing energy
+
SM particle pair

THE NA64 SETUP



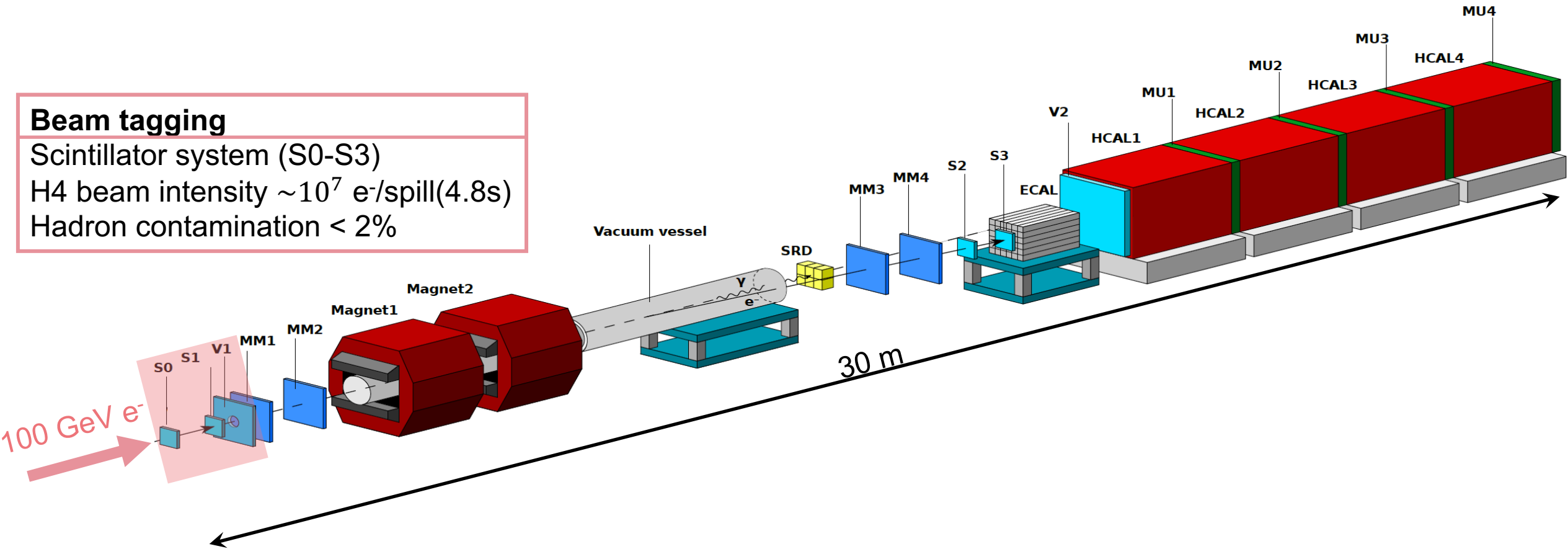
THE NA64 SETUP

Beam tagging

Scintillator system (S0-S3)

H4 beam intensity $\sim 10^7$ e-/spill(4.8s)

Hadron contamination $< 2\%$



THE NA64 SETUP

Momentum reconstruction

Tracking system

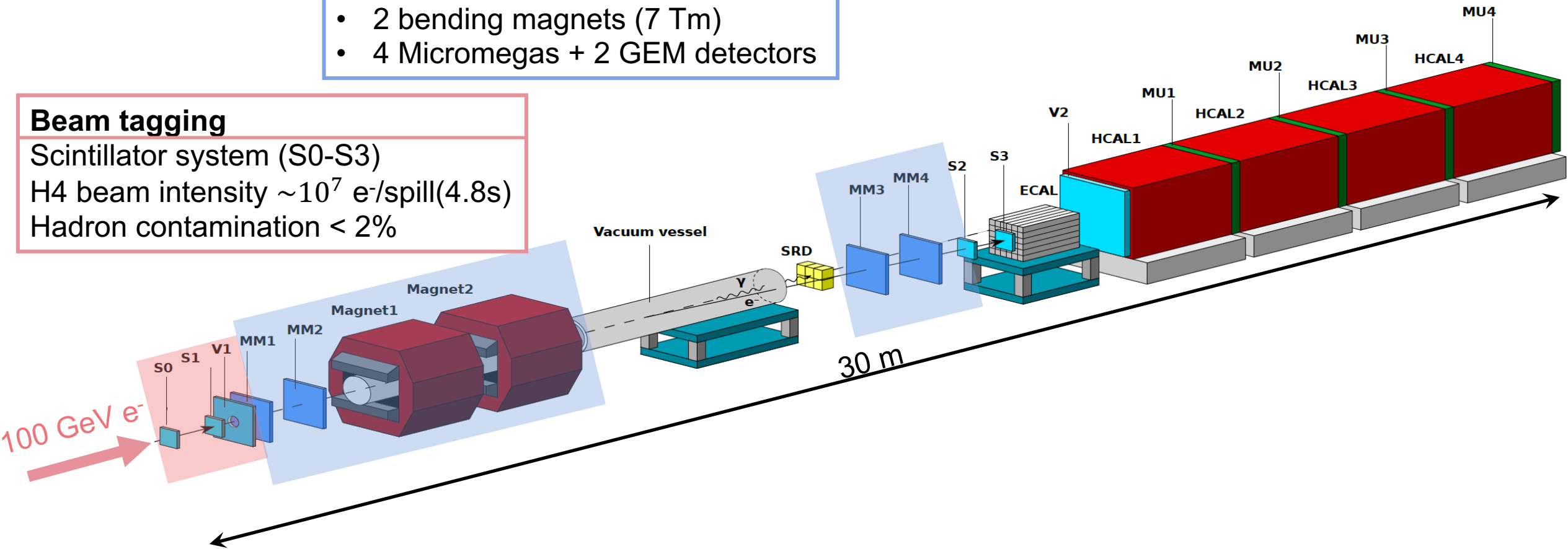
- 2 bending magnets (7 Tm)
- 4 Micromegas + 2 GEM detectors

Beam tagging

Scintillator system (S0-S3)

H4 beam intensity $\sim 10^7$ e-/spill(4.8s)

Hadron contamination $< 2\%$



THE NA64 SETUP

Momentum reconstruction

Tracking system

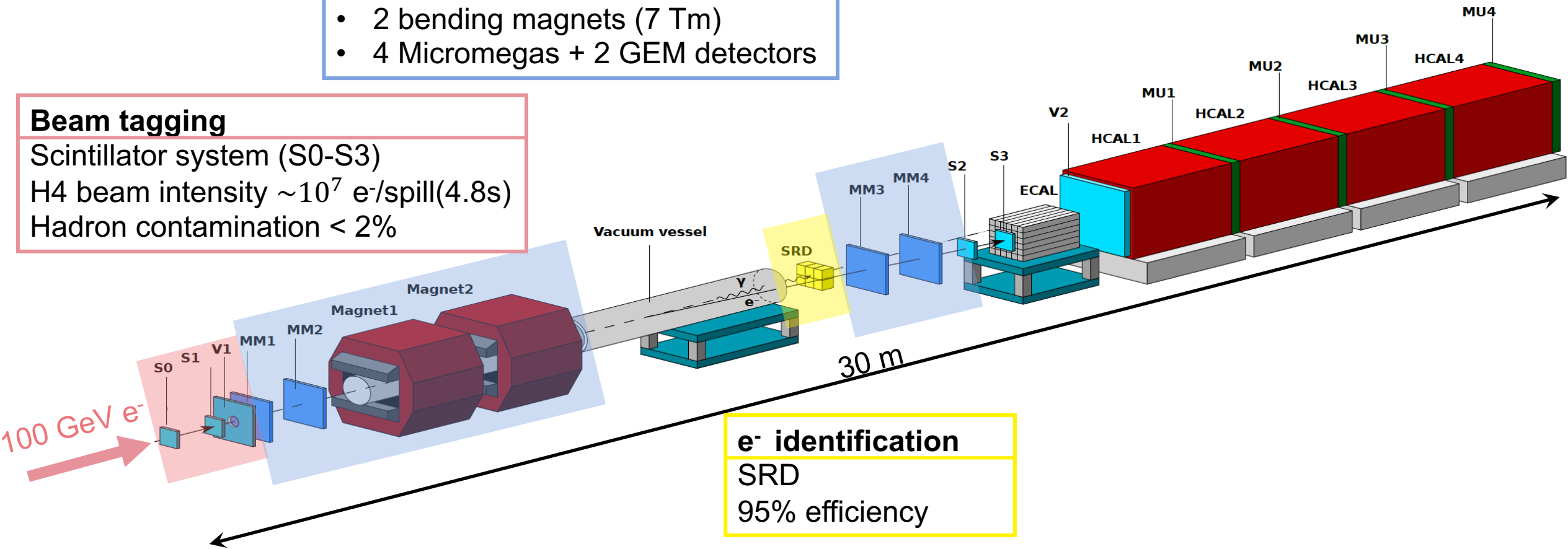
- 2 bending magnets (7 Tm)
- 4 Micromegas + 2 GEM detectors

Beam tagging

Scintillator system (S0-S3)

H4 beam intensity $\sim 10^7$ e-/spill(4.8s)

Hadron contamination < 2%



e^- identification

SRD

95% efficiency

THE NA64 SETUP

Momentum reconstruction

Tracking system

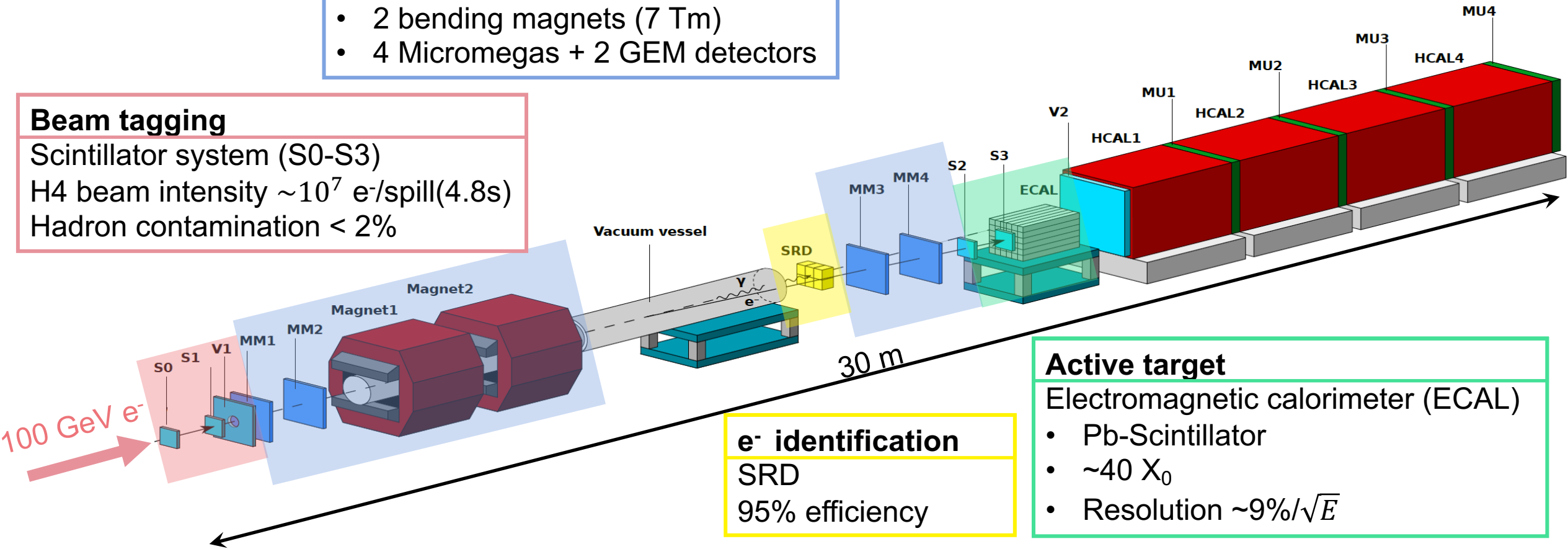
- 2 bending magnets (7 Tm)
- 4 Micromegas + 2 GEM detectors

Beam tagging

Scintillator system (S0-S3)

H4 beam intensity $\sim 10^7$ e-/spill(4.8s)

Hadron contamination $< 2\%$



e^- identification

SRD

95% efficiency

Active target

Electromagnetic calorimeter (ECAL)

- Pb-Scintillator
- $\sim 40 X_0$
- Resolution $\sim 9\%/\sqrt{E}$

THE NA64 SETUP

Momentum reconstruction

Tracking system

- 2 bending magnets (7 Tm)
- 4 Micromegas + 2 GEM detectors

Hermeticity

Veto + Hadronic calorimeter (HCAL)

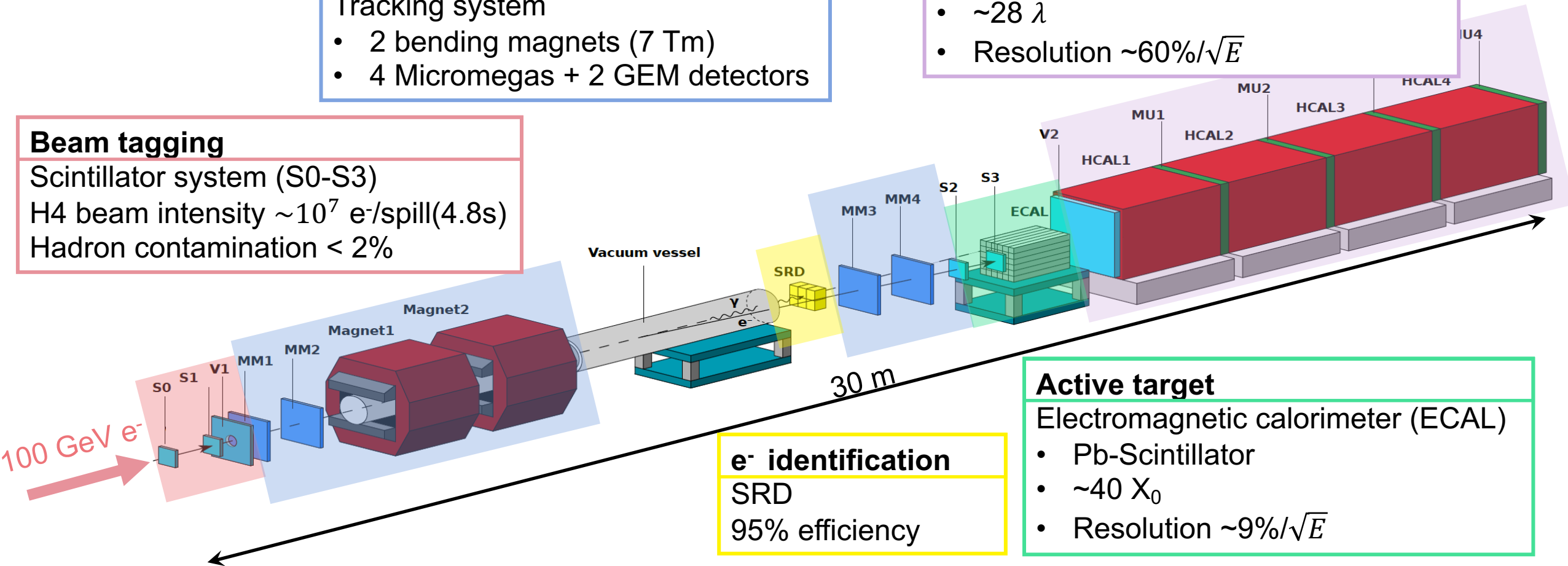
- Fe-Scintillator
- $\sim 28 \lambda$
- Resolution $\sim 60\%/\sqrt{E}$

Beam tagging

Scintillator system (S0-S3)

H4 beam intensity $\sim 10^7$ e-/spill(4.8s)

Hadron contamination $< 2\%$



e^- identification

SRD

95% efficiency

Active target

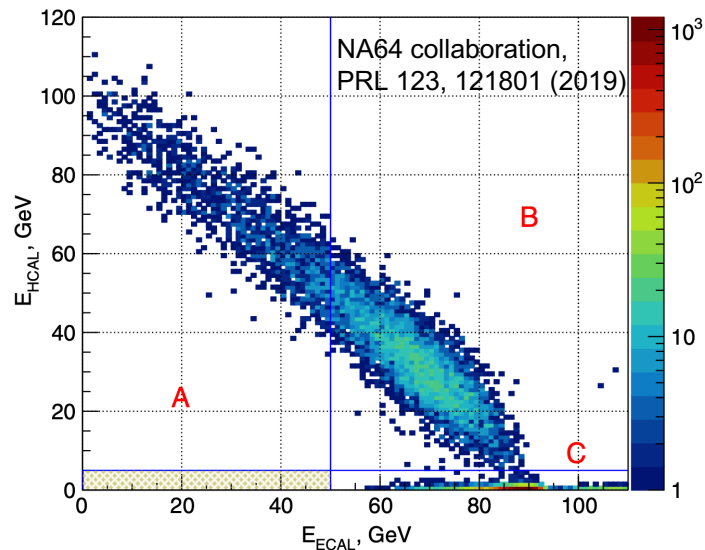
Electromagnetic calorimeter (ECAL)

- Pb-Scintillator
- $\sim 40 X_0$
- Resolution $\sim 9\%/\sqrt{E}$

INVISIBLE ANALYSIS

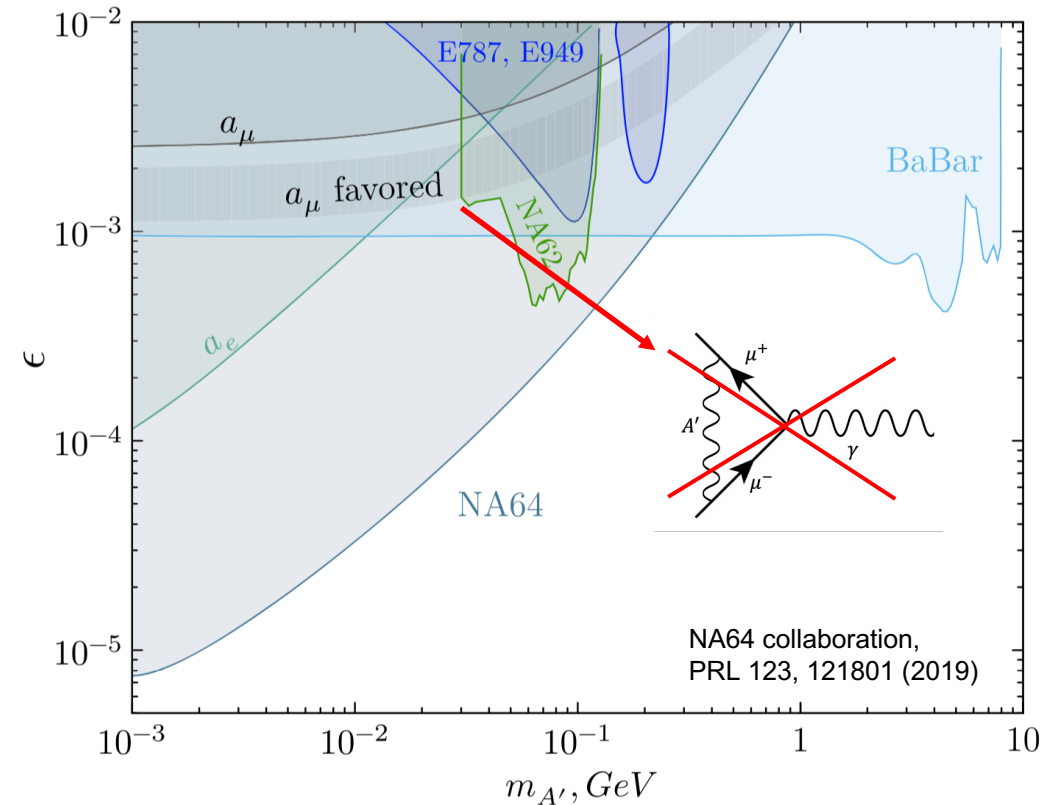
Event selection:

- Timing information: pile-up and noise suppression
- Clean incoming 100 GeV track: momentum reconstruction
- e^- identification: SRD + ECAL shower profile
- Hadrons rejection: no activity in VETO and HCAL



Signal region: $E_{\text{ECAL}} < 50$ GeV, $E_{\text{HCAL}} < 1$ GeV

Data collected in 2016-2018 ($2.84 \cdot 10^{11}$ EOT)



Recasted on iDM and i2DM

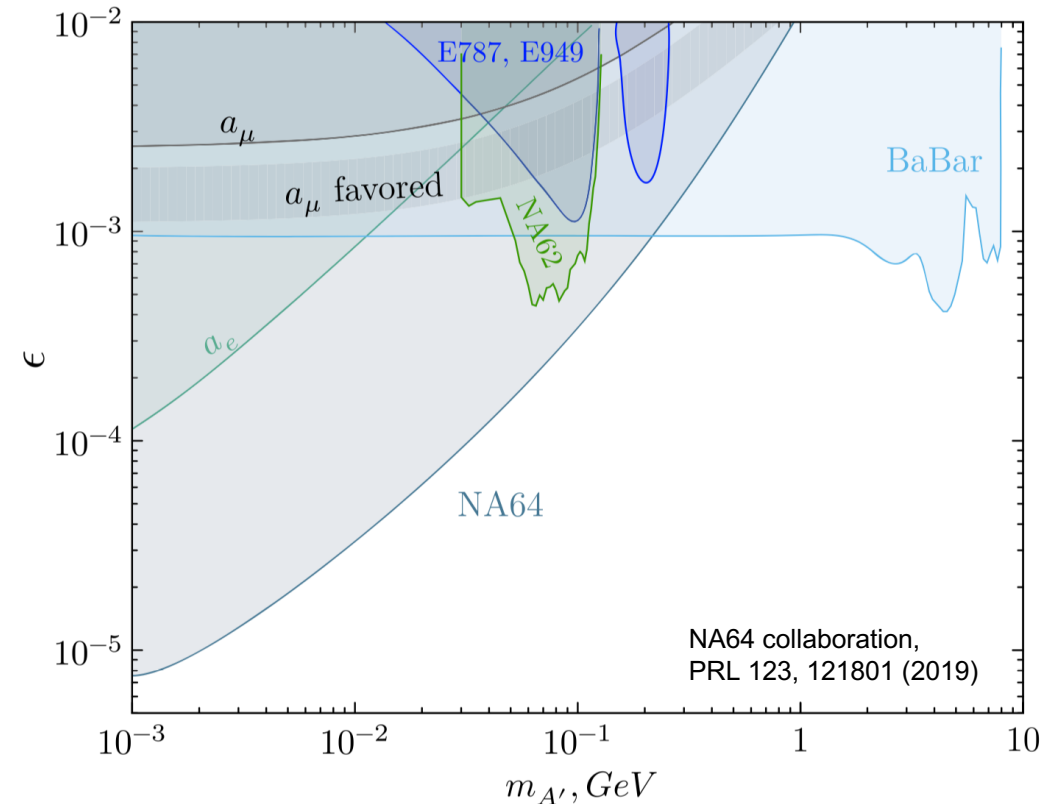
SEMI-VISIBLE RECAST ANALYSIS

Recast of the invisible limits:

- Selection criteria: invisible analysis cutflow
- Statistics: $2.84 \cdot 10^{11}$ e^- on target (EOT)
- Signal MC: Bremsstrahlung A' production, grid simulations using Geant4 and DMG4 M. Bondi et al. CPC 269, 108129 (2021)
- Signal efficiency: Selection efficiency on data + cutflow on signal simulation
- Background expectation: (0.53 ± 0.17) events
- Constraints: 90% C.L. exclusion limits, background-free hypothesis

Signal region: $ECAL < 50$ GeV, $HCAL < 1$ GeV

Data collected in 2016-2018 ($2.84 \cdot 10^{11}$ EOT)



Recasted on iDM and i2DM

SEMI-VISIBLE RECAST ANALYSIS

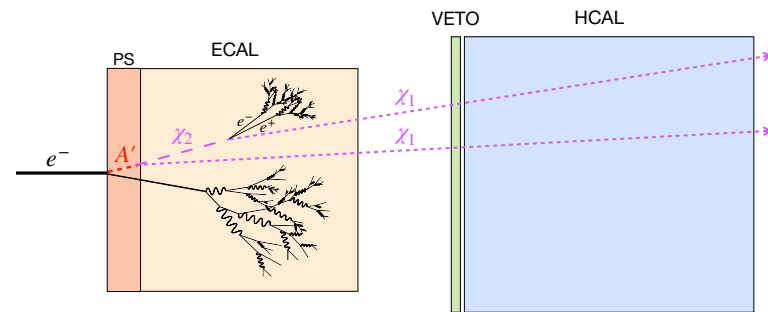
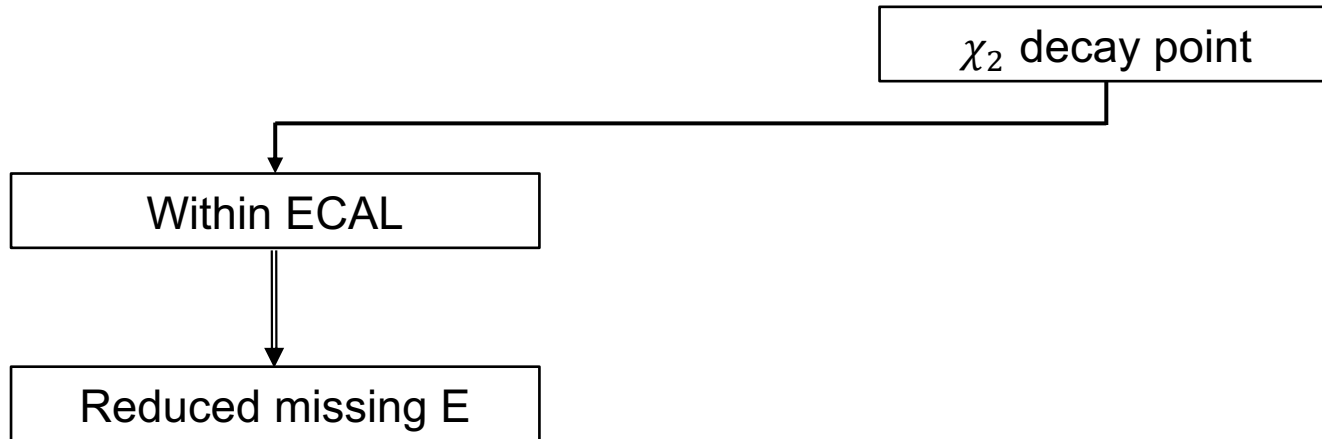
Difference w.r.t. invisible scenario: e^-e^+ **visible energy deposit** $\Gamma(\chi_2 \rightarrow \chi_1 f \bar{f}) \sim \frac{4\epsilon^2 \alpha \alpha_D \Delta^5}{15\pi m_{A'}^4}$ $\tau_{\chi_2} \propto \frac{1}{\epsilon^2 m_{A'}}$

→ Depending on the parameter settings, **3 main regimes** can be distinguished:

SEMI-VISIBLE RECAST ANALYSIS

Difference w.r.t. invisible scenario: e^-e^+ **visible energy deposit** $\Gamma(\chi_2 \rightarrow \chi_1 f \bar{f}) \sim \frac{4\epsilon^2 \alpha \alpha_D \Delta^5}{15\pi m_{A'}^4}$ $\tau_{\chi_2} \propto \frac{1}{\epsilon^2 m_{A'}}$

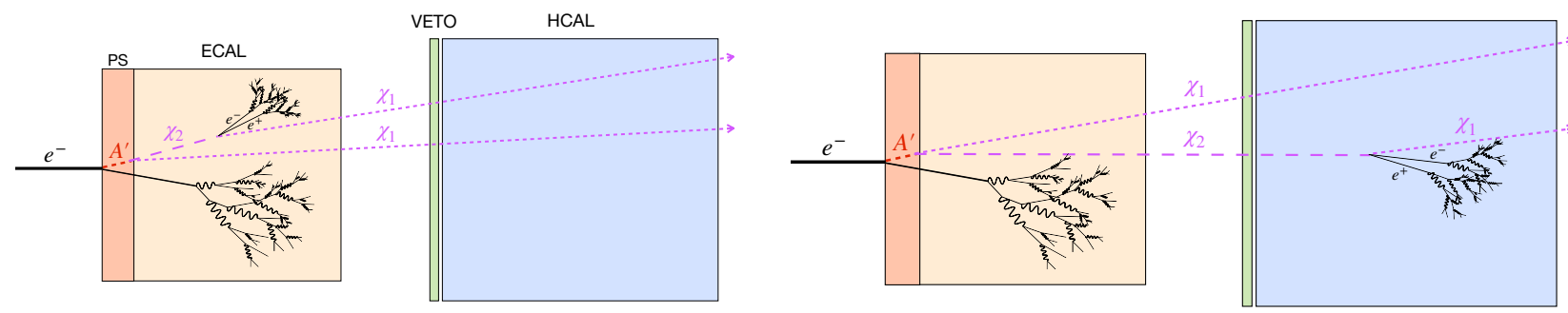
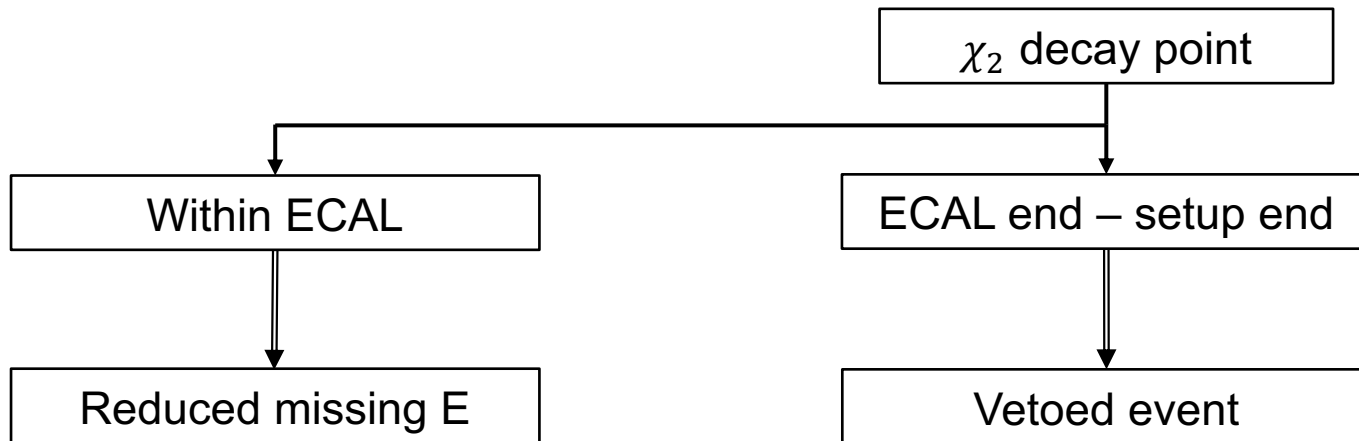
→ Depending on the parameter settings, **3 main regimes** can be distinguished:



SEMI-VISIBLE RECAST ANALYSIS

Difference w.r.t. invisible scenario: e^-e^+ **visible energy deposit** $\Gamma(\chi_2 \rightarrow \chi_1 f \bar{f}) \sim \frac{4\epsilon^2 \alpha \alpha_D \Delta^5}{15\pi m_{A'}^4}$ $\tau_{\chi_2} \propto \frac{1}{\epsilon^2 m_{A'}}$

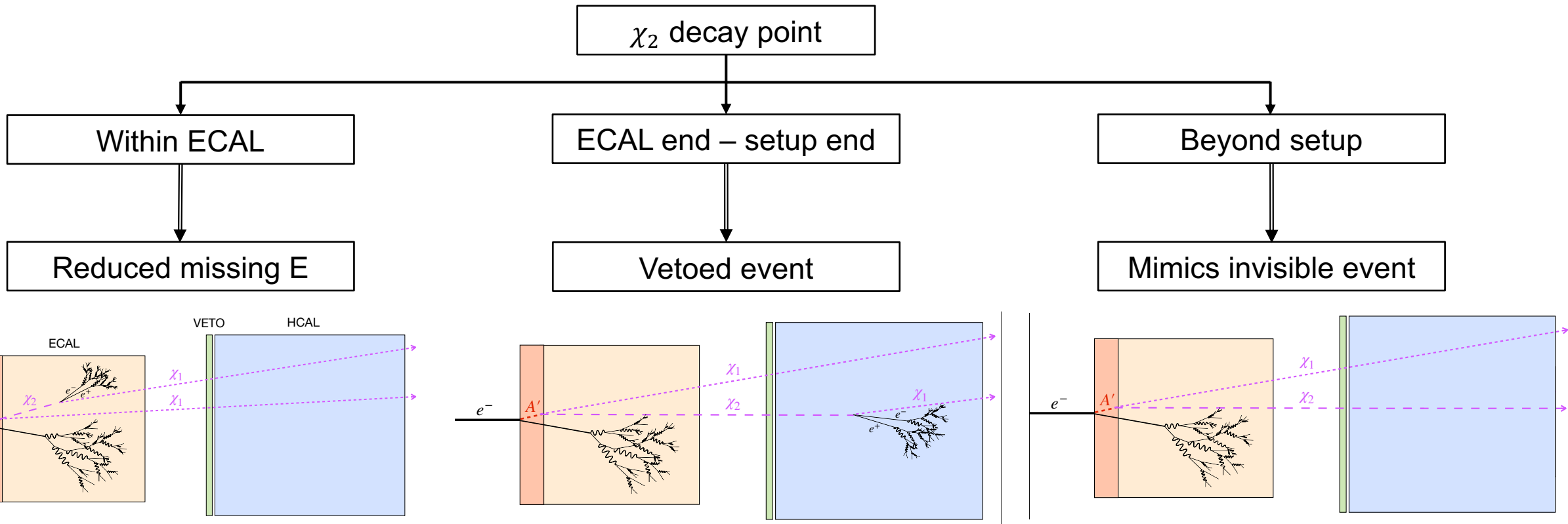
→ Depending on the parameter settings, **3 main regimes** can be distinguished:



SEMI-VISIBLE RECAST ANALYSIS

Difference w.r.t. invisible scenario: e^-e^+ **visible energy deposit** $\Gamma(\chi_2 \rightarrow \chi_1 f \bar{f}) \sim \frac{4\epsilon^2 \alpha \alpha_D \Delta^5}{15\pi m_{A'}^4}$ $\tau_{\chi_2} \propto \frac{1}{\epsilon^2 m_{A'}}$

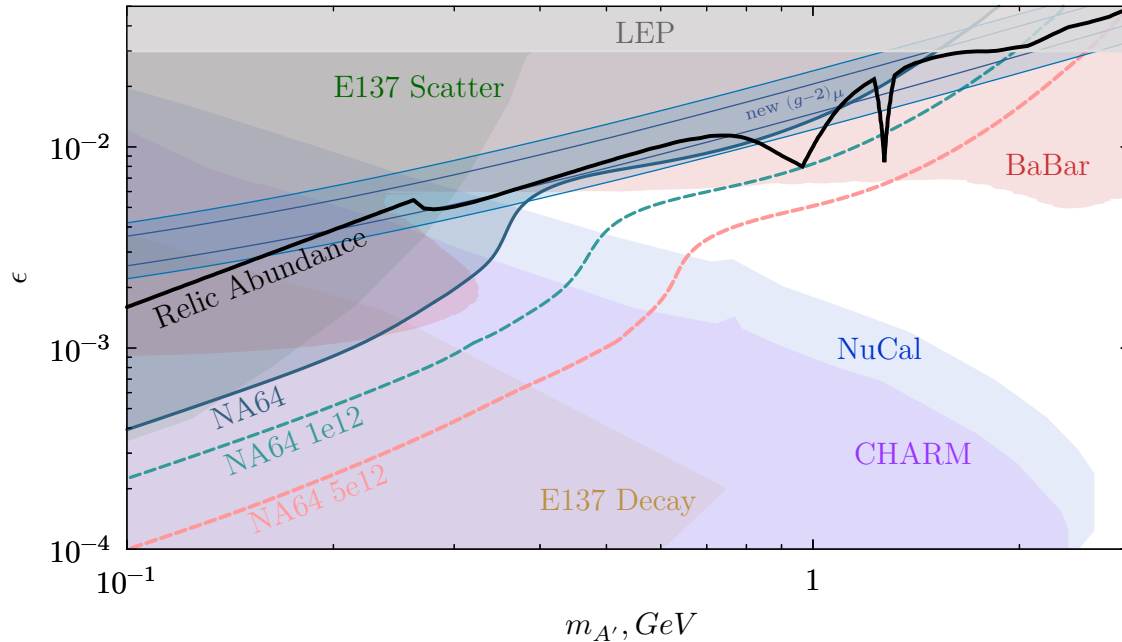
→ Depending on the parameter settings, **3 main regimes** can be distinguished:



RESULTS – FOCUS ON $(g - 2)_\mu$

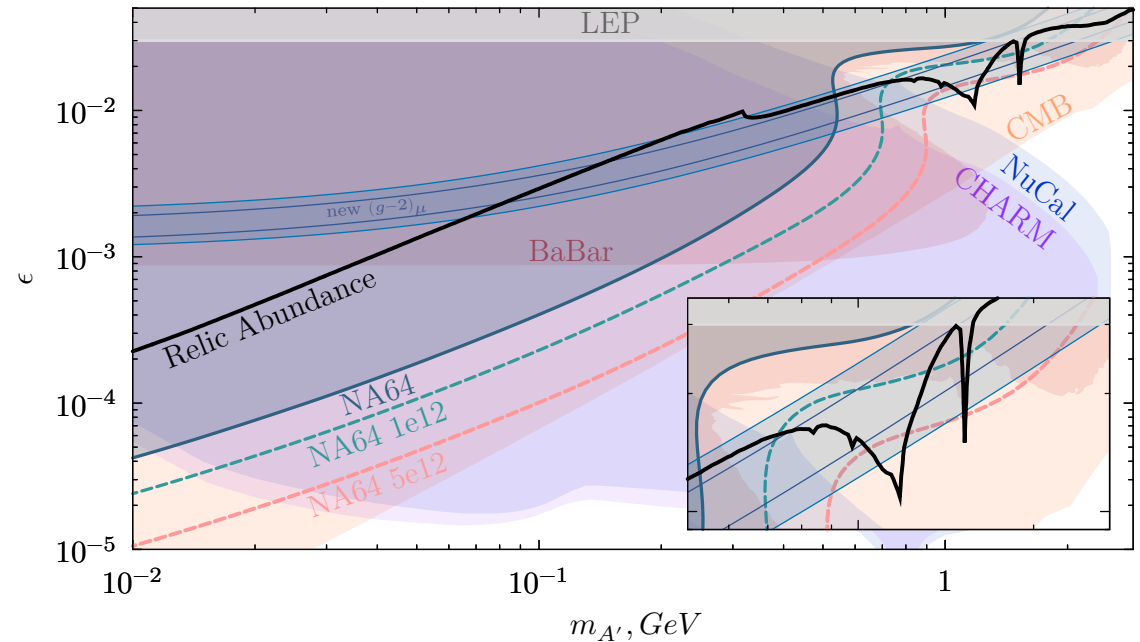
iDM

$$\Delta = 0.4m_{\chi_1}, m_A = 3m_{\chi_1}, \alpha_D = 0.1$$



i2DM

$$\text{i2DM, } \Delta = 0.4m_{\chi_1}, m_A = 3m_{\chi_1}, \alpha_D = 0.5, \theta = 0.08$$



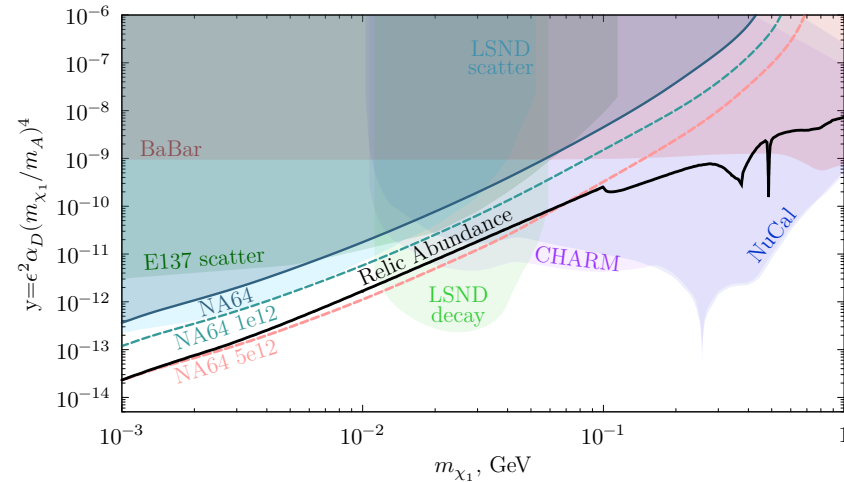
- Large mass splitting \rightarrow increased energy in visible final state \rightarrow loosening of the constraints
- Both iDM and i2DM **are excluded** as viable explanation of the $(g - 2)_\mu$ anomaly
 - \rightarrow NA64 and BaBar play a central role
 - \rightarrow i2DM tightly constrained by CMB

M. Mongillo et al.,
EPJ C 83, 391 (2023)

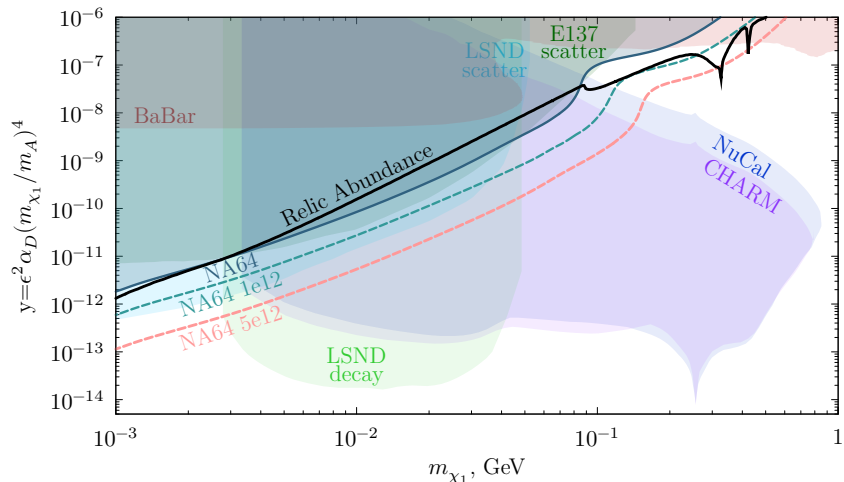
THERMAL RELIC TARGET – IDM

iDM

Thermal iDM, $\Delta = 0.1m_{\chi_1}, m_A = 3m_{\chi_1}, \alpha_D = 0.1$

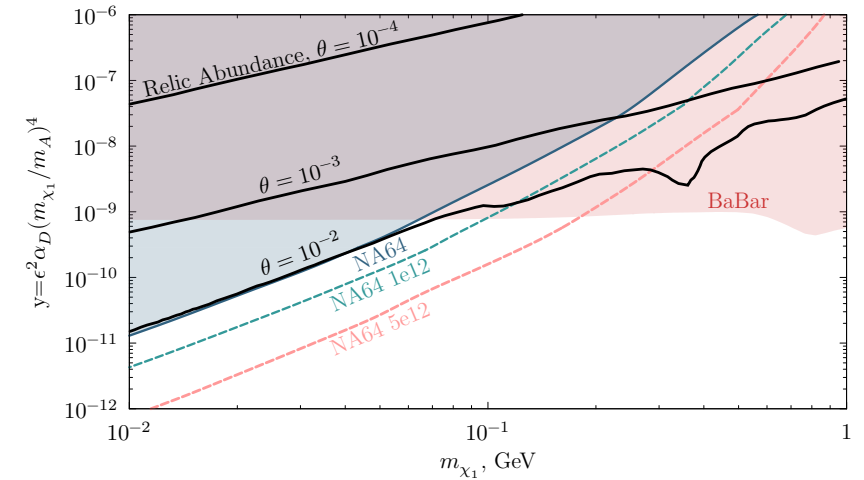


Thermal iDM, $\Delta = 0.4m_{\chi_1}, m_A = 3m_{\chi_1}, \alpha_D = 0.5$

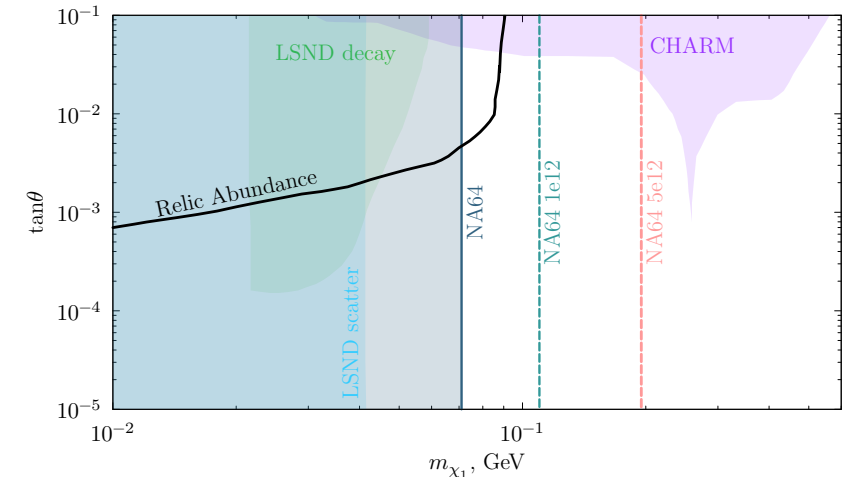


i2DM

i2DM, $\Delta = 0.05m_{\chi_1}, m_A = 3m_{\chi_1}, \alpha_D = 1/(4\pi)$



i2DM, $\Delta = 0.05m_{\chi_1}, \epsilon = 0.001, m_A = 3m_{\chi_1}, \alpha_D = 1/(4\pi)$



Projections in $m_{\chi_1} - y$ and $m_{\chi_1} - \tan \theta$ planes:

- Some relic target region remains to be tested for both models
- With $5 \cdot 10^{12}$ EOT: large coverage of the DM targets for different parametrizations in MeV-GeV range

M. Mongillo et al.,
EPJ C 83, 391 (2023)

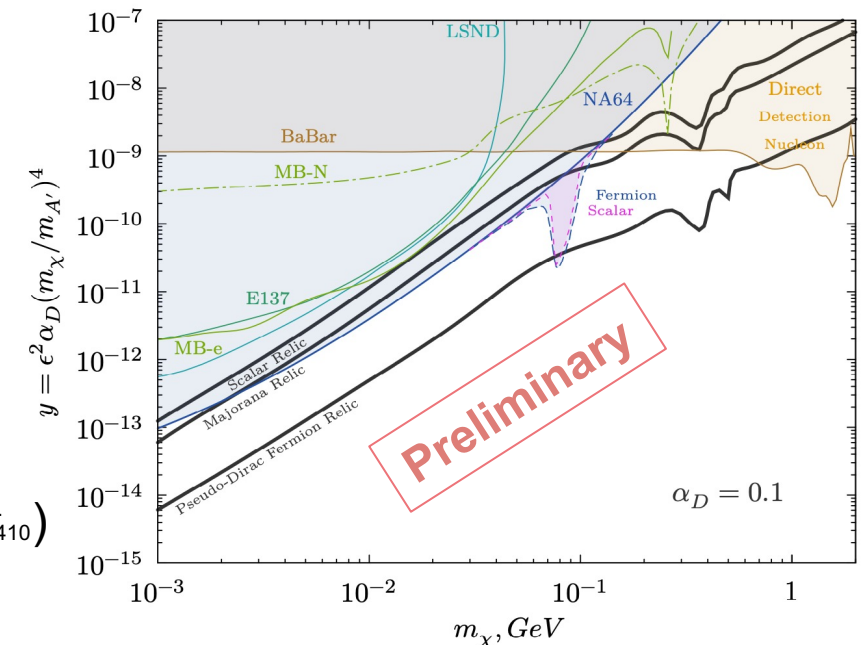
CONCLUSIONS AND OUTLOOK

- NA64 is a **powerful probe** of semi-visible dark photons
- **New limits** were obtained on regions of parameter space characterized by prompt χ_2 decays
- Most of the parameter space favoured for $(g - 2)_\mu$ **discrepancy has been excluded** for both the iDM and i2DM
- With the statistics expected before LS3, **NA64 can test the thermal targets** for iDM and i2DM in MeV-GeV range

What is next?

- Analysis of the 2022 and 2023 data
- Displaced vertex search
- Inclusion of the A' resonant annihilation production
- Extension to other semi-visible models (e.g. HNL models)
- Setup optimization study

Abdullahi et al.
arXiv:2302.05410



CONCLUSIONS AND OUTLOOK

Thank you!



Acknowledgments

NA64 collaboration

ETH Zürich group: P. Crivelli, B. Banto Oberhauser, E. Depero, H. Sieber

IFIC group: L. Molina Bueno, M. Tuzi

A. Abdullahi, M. Hostert, D. Massaro, S. Pascoli

BACKUP SLIDES

DARK SECTORS

Dark particles could interact via **new feeble interactions**, generating portal connections with the SM

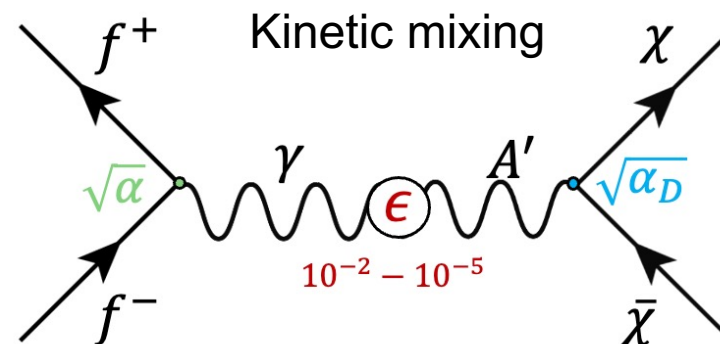
Renormalizable portals:

- **Vector portal** → **dark photon**
- Scalar portal → dark Higgs
- Fermion portal → heavy neutral leptons



Vector portal: addition of new $U(1)_D$ symmetry to the SM gauge group

$$\rightarrow \mathcal{L}_{DP} = \frac{m_{A'}^2}{2} A'_\mu A'^\mu + A'_\mu (g_D J_{DS}^\mu - e\epsilon J_{EM}^\mu)$$



DARK SECTORS

Dark particles could interact via **new feeble interactions**, generating portal connections with the SM

Renormalizable portals:

- **Vector portal** → **dark photon**
- Scalar portal → dark Higgs
- Fermion portal → heavy neutral leptons



Motivations: known gaps in SM + experimental anomalies

- Sub-GeV thermal dark matter
- Neutrino masses generation
- Muon $(g - 2)_\mu$ anomaly

DM abundance

$$\Omega_\chi \propto \frac{1}{\langle \sigma v \rangle} \approx 0.24$$
$$\sigma v(\chi\chi \rightarrow A'^* \rightarrow ff) \propto \epsilon^2 \alpha_D \frac{m_\chi^2}{m_{A'}^4} = \frac{y}{m_\chi^2}$$

THE MUON $(g - 2)_\mu$ PUZZLE

2002: E821 experiment at BNL $\rightarrow 3.7\sigma$ discrepancy
 2021: E989 experiment at FNAL \rightarrow increased discrepancy to 4.2σ
 Next: experiment at J-PARC

SM prediction: $a_\mu^{SM} = a_\mu^{QED} + a_\mu^{EW} + a_\mu^{Had}$

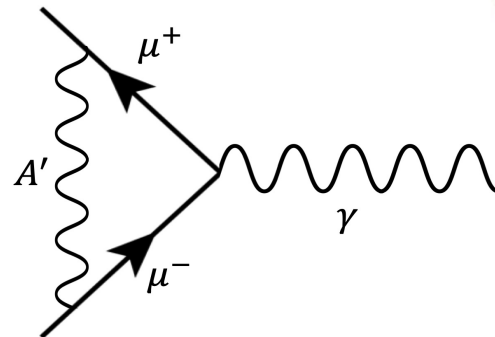
\rightarrow data-driven traditional method

\rightarrow lattice QCD

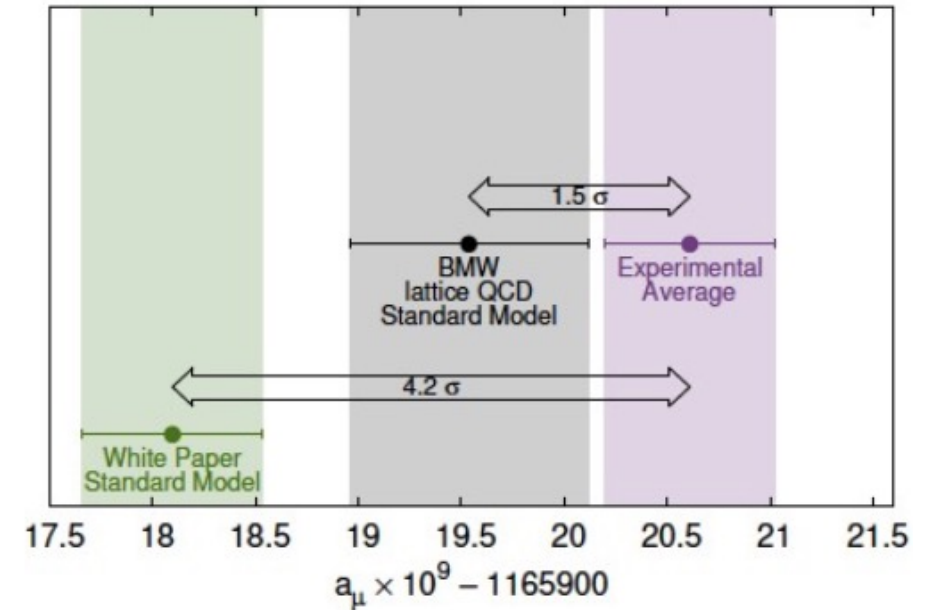
$\curvearrowright 2.1\sigma$

Dark photon contribution:

$$a_\mu^{A'} = \frac{\alpha}{2\pi} \varepsilon^2 F\left(m_{A'}/m_\mu\right)$$

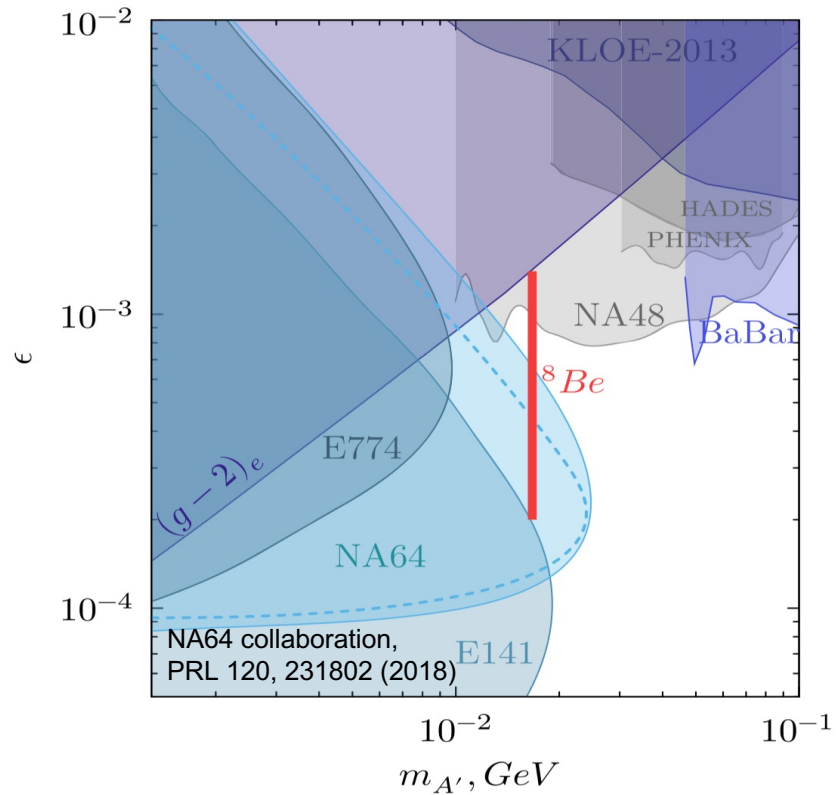


$$a_\mu = \frac{g_\mu - 2}{2}$$

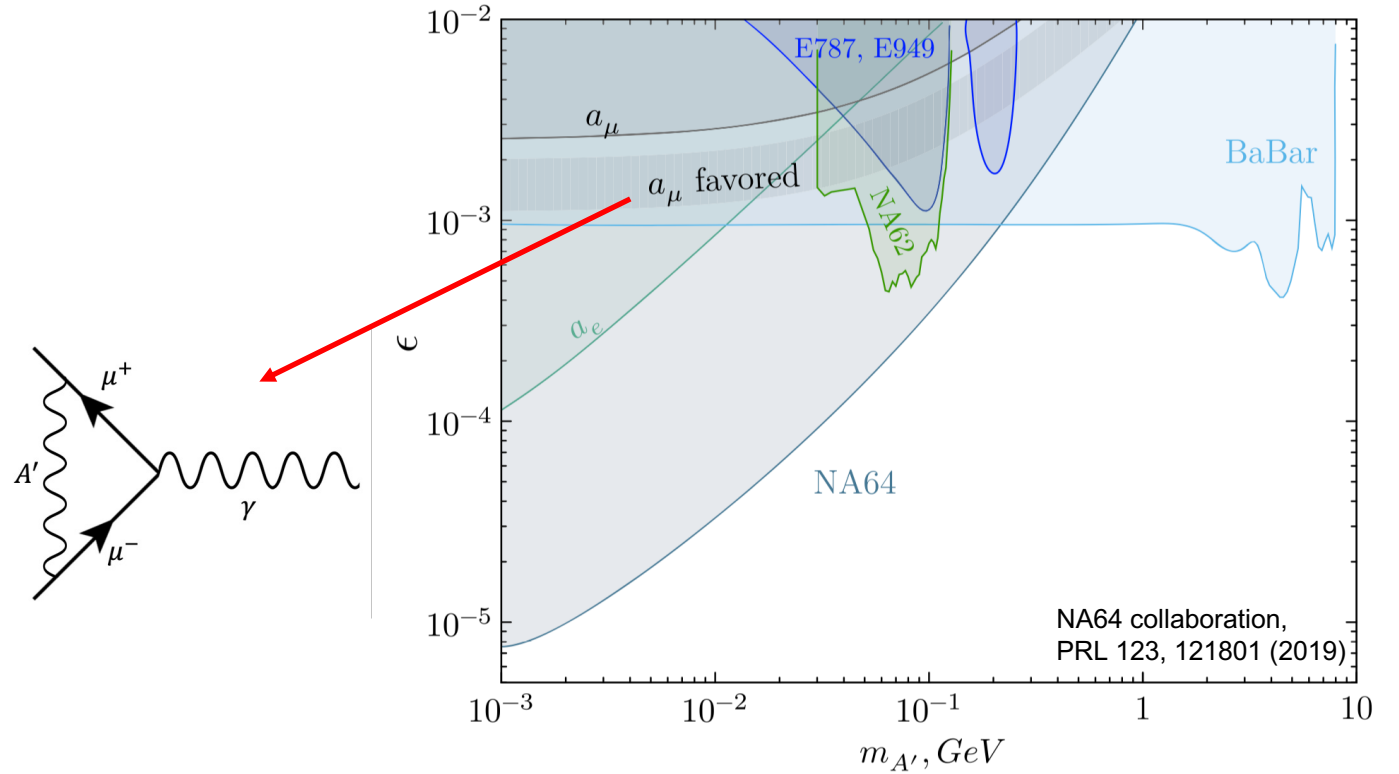


VISIBLE AND INVISIBLE DARK PHOTON DECAYS

Visible decay mode



Invisible decay mode



→ Both decay modes had been excluded experimentally as explanations of the $(g - 2)_\mu$ discrepancy

RECAST INVISIBLE ANALYSIS RESULTS

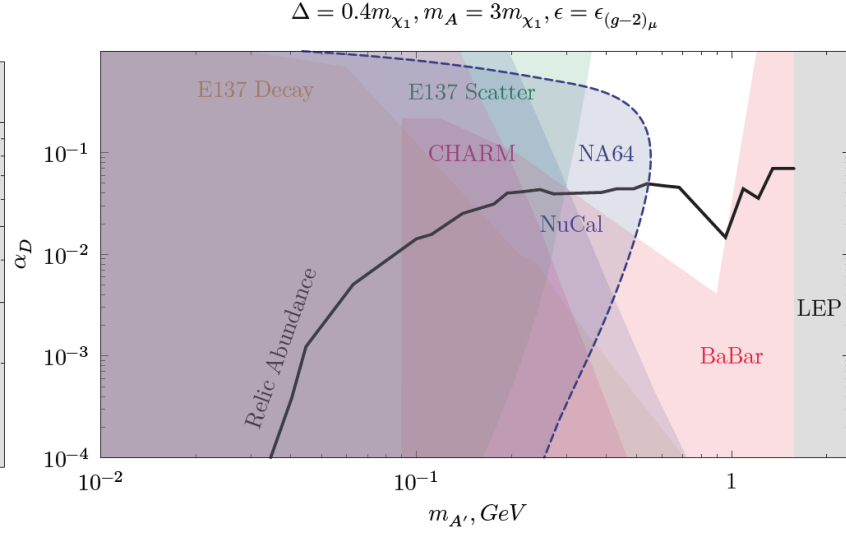
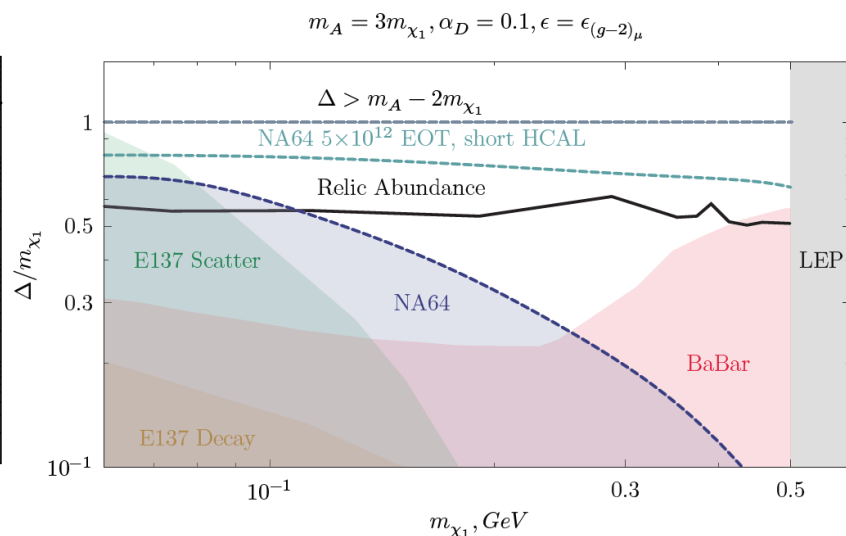
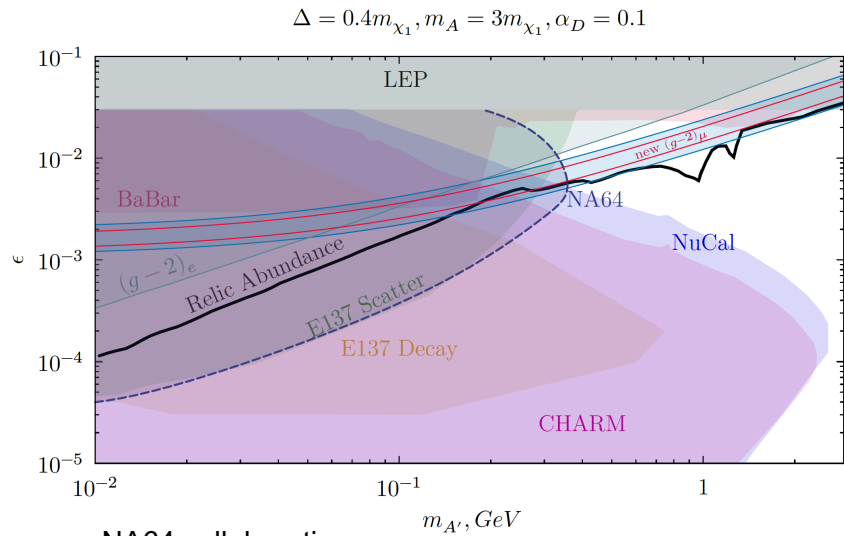
- Projections show that these semi-visible models are within the reach of the experiment even without dedicated modifications in the analysis techniques → reinterpret the invisible analysis bounds obtained with the 2016-2018 statistics

Procedure:

1. Simulate many parameter space points $(m_{A'}, \epsilon)$ for each model (grid of 80x80 points)
2. Apply relevant cuts for semi-visible signals on MC simulations (all the cuts effective from the point where A' could potentially be produced) → cut values taken from invisible analysis
3. Correct accumulated EOT with total efficiency obtained from the entire list of cuts applied in the invisible analysis (these efficiency were estimated on electron calibration runs)
4. Given that the calculated boundaries were basically unaltered when considering the expected background, the limits were calculated with a background-free hypothesis, excluding a specific parameter if: $N_{A'}/EOT \cdot EOT \geq 2.3$

	2016 I	2016 II	2016 III	2017	2018
EOT 10^{10}	2.3	1.1	0.9	5.4	19
Efficiency	0.7	0.841	0.786	0.55	0.5
Effective EOT 10^{10}	1.61	0.92	0.71	3	9.5
BKG	0.0097	0.0088	0.002	0.237	0.215

STARTING POINT – IDM PUBLICATION (2021)

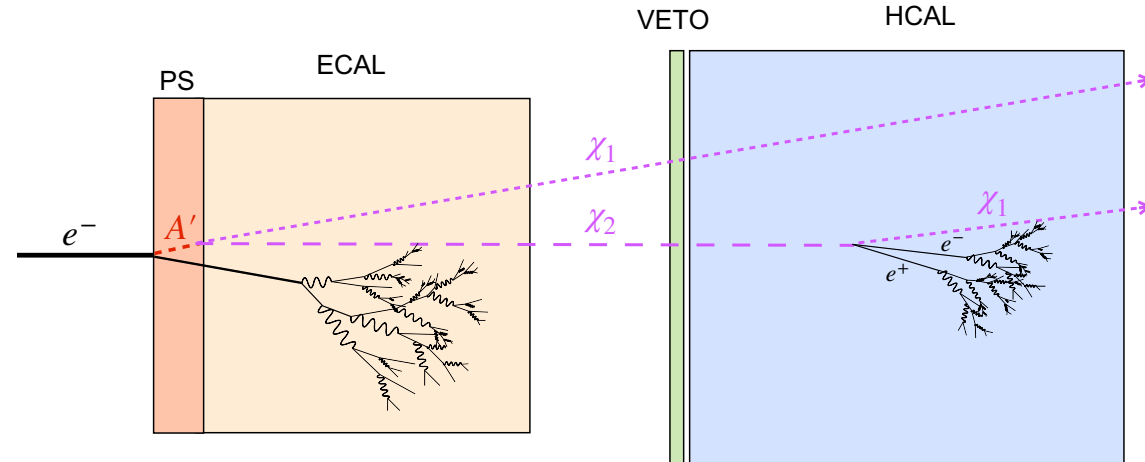


NA64 collaboration, EPJ C 81, 959 (2021)

Signal event definition:

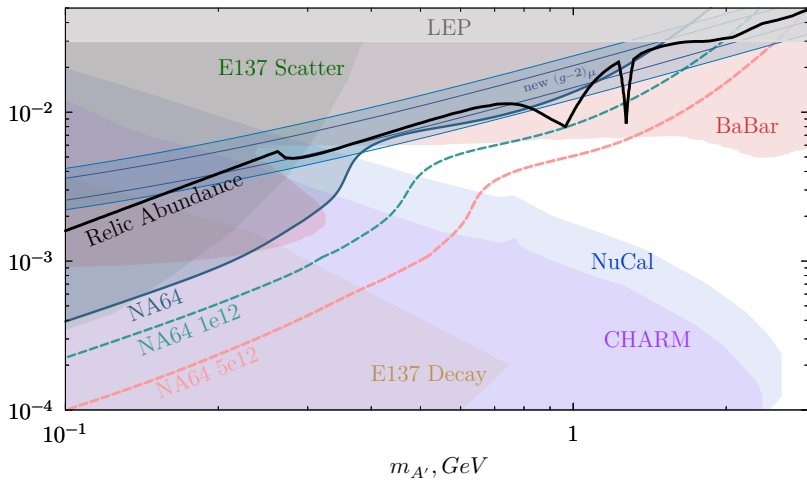
- χ_2 decays in HCAL2 or HCAL3 → **Displaced vertex**
- χ_2 decays after setup → **Fully invisible signature**

→ Search targeting only long-lived χ_2 ($d_{\chi_2} \gtrsim 2.5$ m)

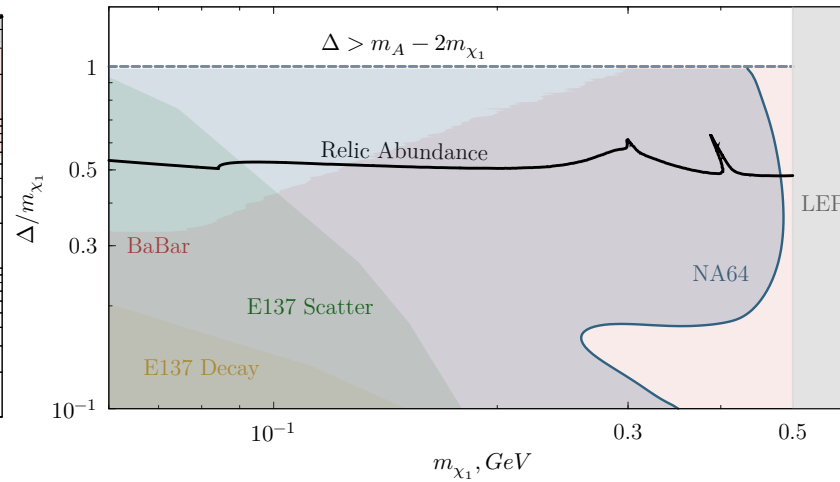


NEW RESULTS ON IDM – FOCUS ON $(g - 2)_\mu$

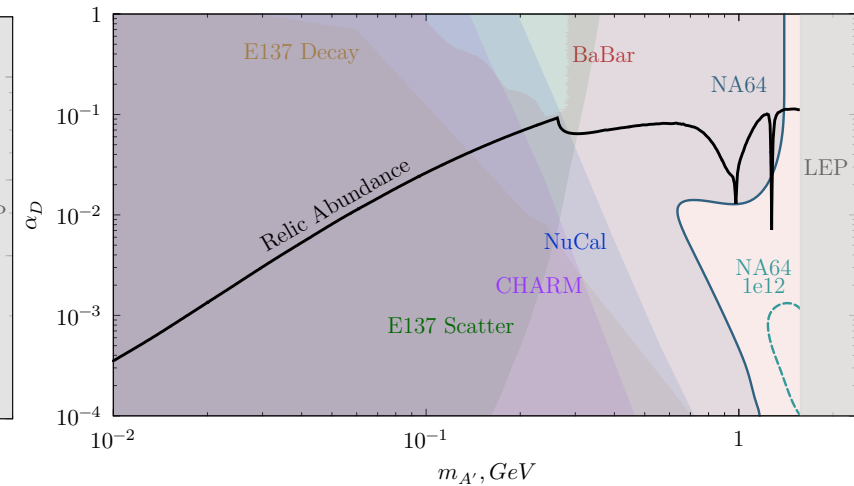
$$\Delta = 0.4m_{\chi_1}, m_A = 3m_{\chi_1}, \alpha_D = 0.1$$



$$m_A = 3m_{\chi_1}, \alpha_D = 0.5, \epsilon = \epsilon_{(g-2)_\mu}$$



$$\Delta = 0.4m_{\chi_1}, m_A = 3m_{\chi_1}, \epsilon = \epsilon_{(g-2)_\mu}$$

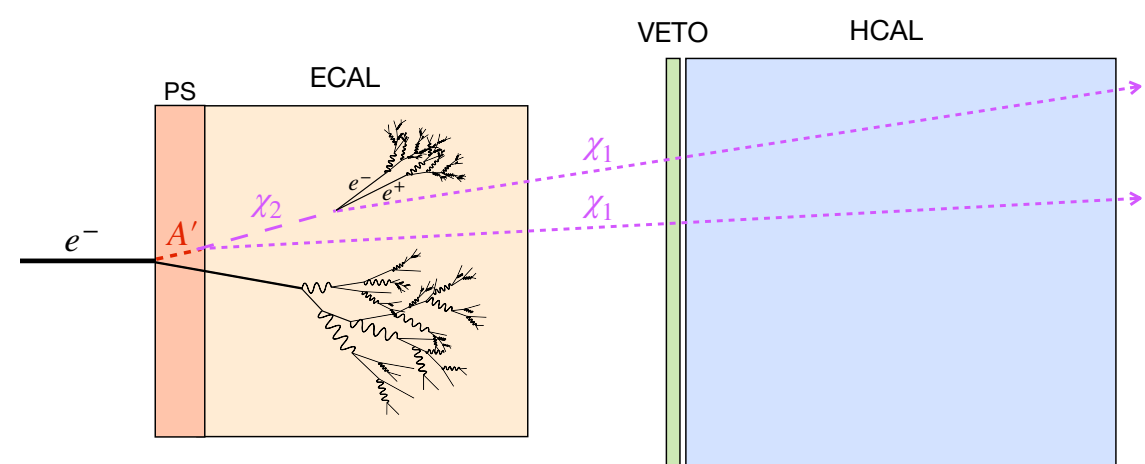


NA64 collaboration,
EPJ C 81, 959 (2021)

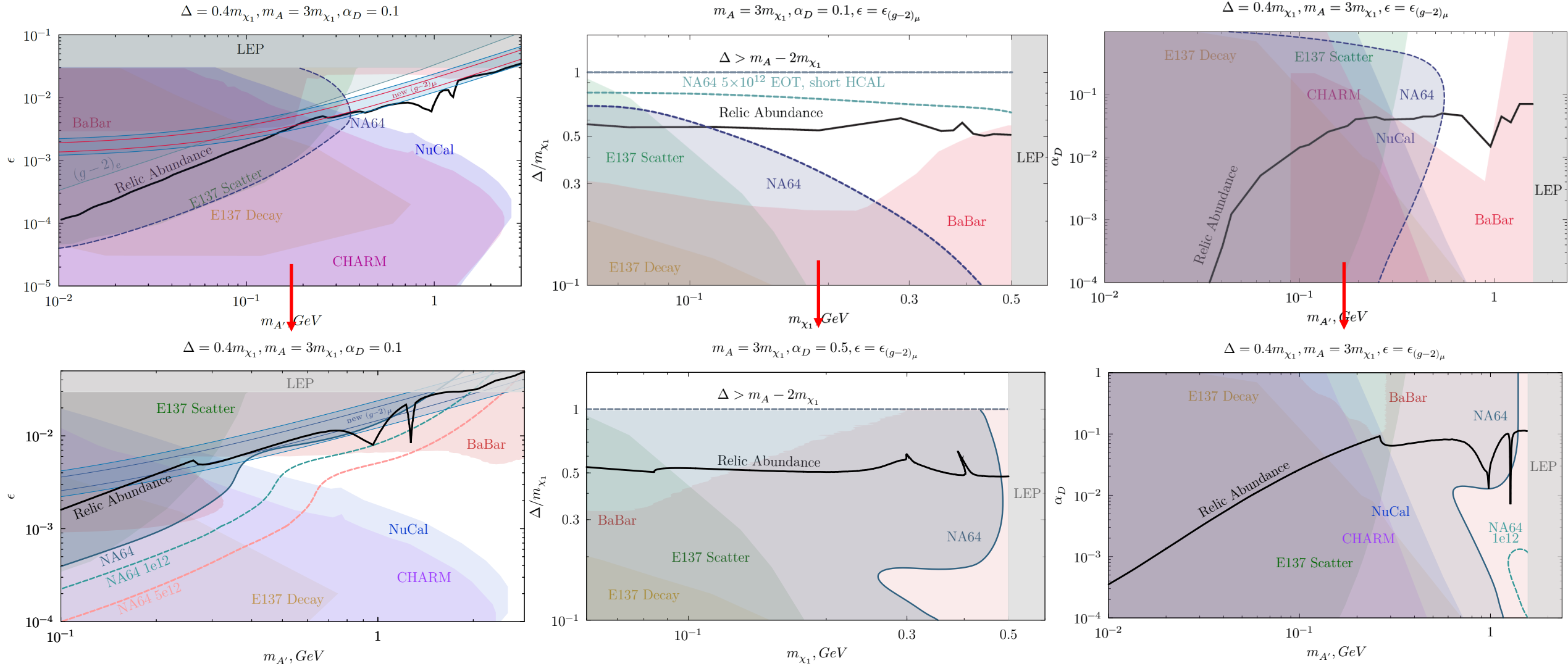
Signal event definition:

- Invisible signature (regardless of the χ_2 decay position)
ECAL < 50 GeV, HCAL < 1 GeV

→ both short and **long-lived** χ_2

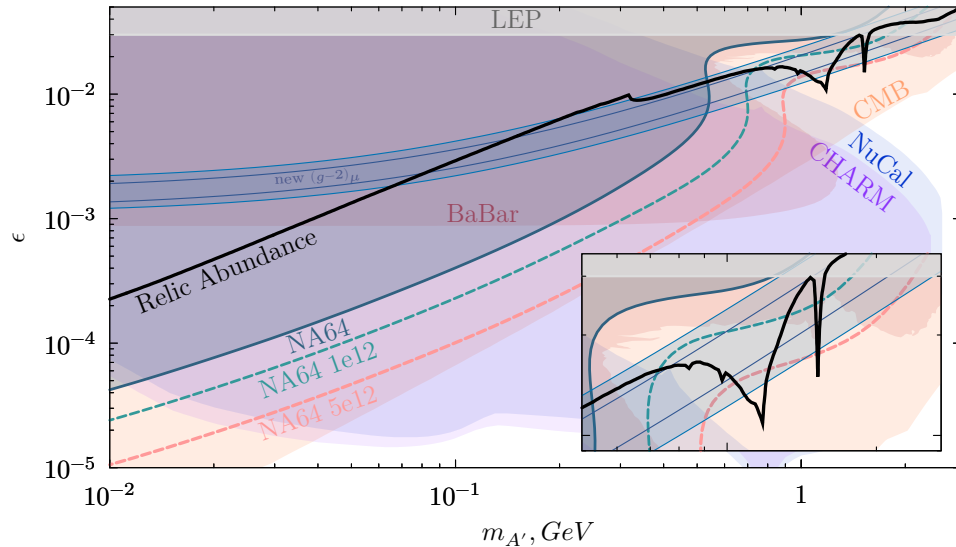


COMPARISON OF THE TWO SEARCHES

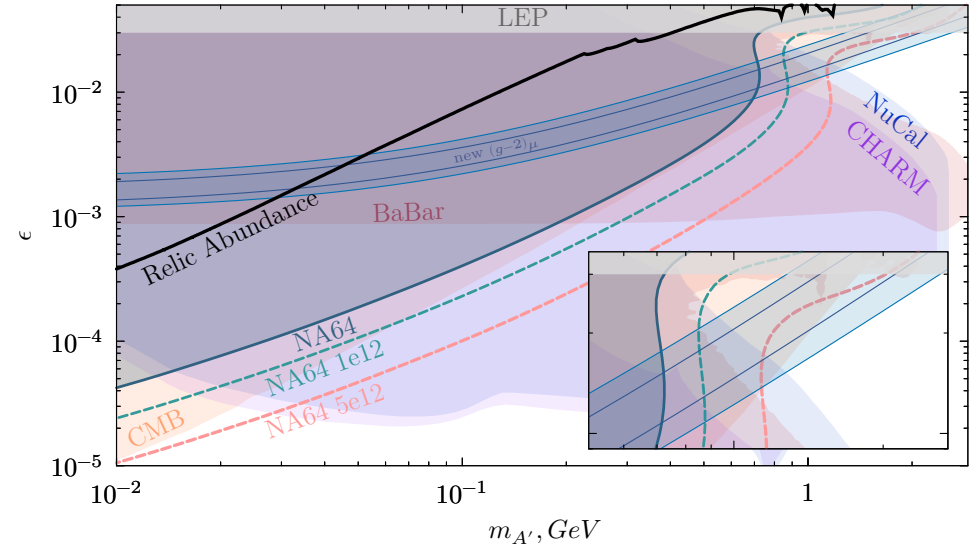


i2DM – FOCUS ON $(g - 2)_\mu$

i2DM, $\Delta = 0.4m_{\chi_1}, m_A = 3m_{\chi_1}, \alpha_D = 0.5, \theta = 0.08$



i2DM, $\Delta = 0.4m_{\chi_1}, m_A = 3m_{\chi_1}, \alpha_D = 0.5, \theta = 0.04$



- Smaller mixing (parametrized by θ) \rightarrow suppressed χ_1 self-annihilation \rightarrow loosen CMB bounds
BUT
- Smaller mixing \rightarrow suppressed cospattering and annihilations \rightarrow overabundant scenario

\rightarrow Both iDM and i2DM are excluded as viable explanation of the $(g - 2)_\mu$ anomaly

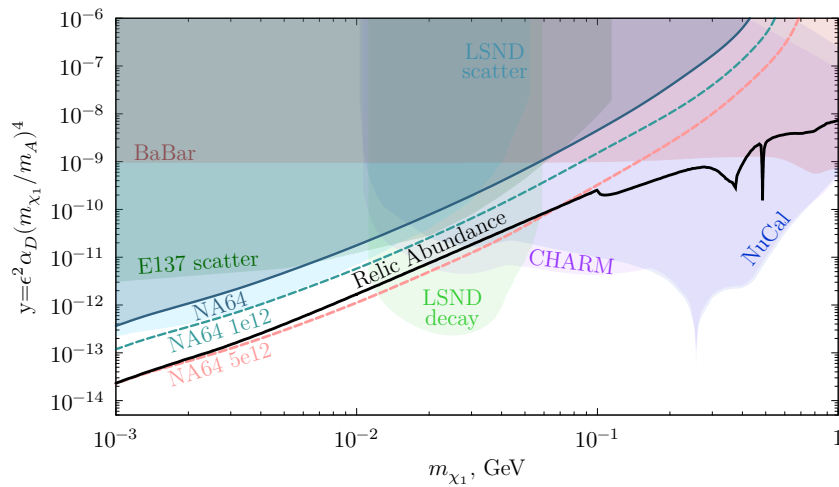
$$Br(A' \rightarrow \chi_1 \chi_1) \propto \sin^4 \theta,$$

$$Br(A' \rightarrow \chi_1 \chi_2) \propto \sin^2 \theta \cos^2 \theta,$$

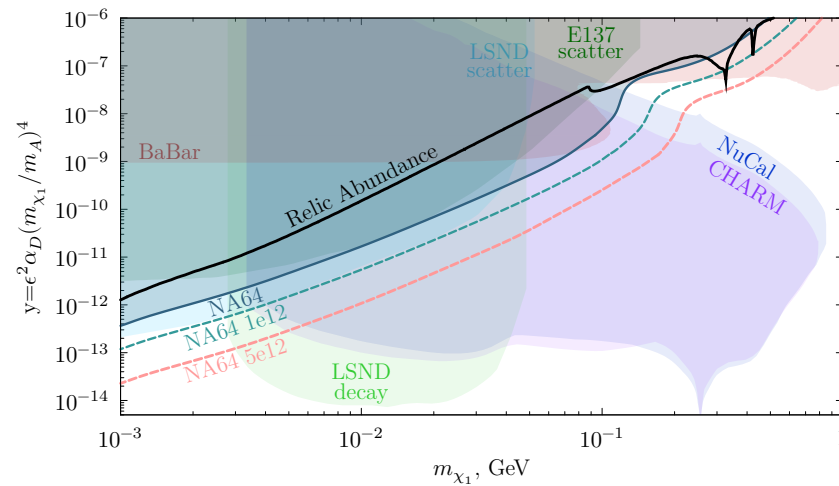
$$Br(A' \rightarrow \chi_2 \chi_2) \propto \cos^4 \theta,$$

THERMAL RELIC TARGET – IDM

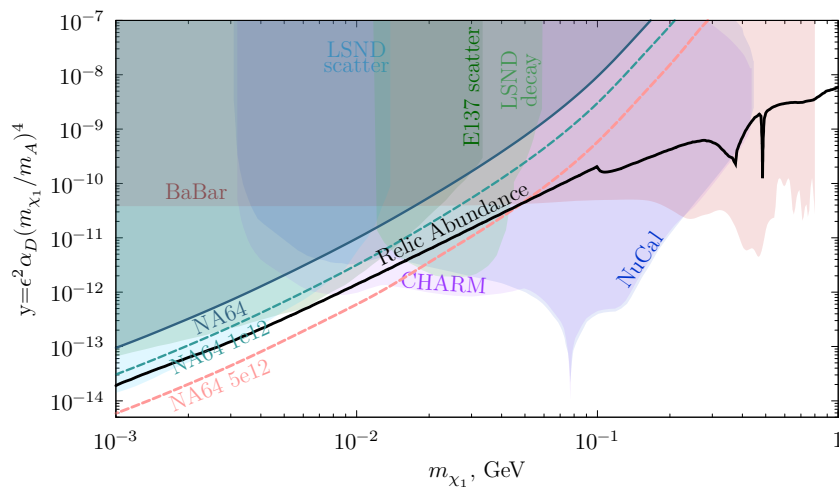
Thermal IDM, $\Delta = 0.1m_{\chi_1}, m_A = 3m_{\chi_1}, \alpha_D = 0.1$



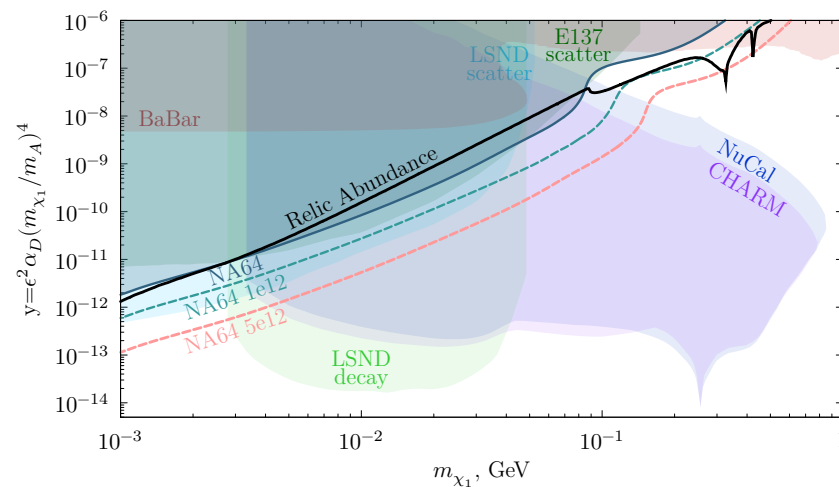
Thermal IDM, $\Delta = 0.4m_{\chi_1}, m_A = 3m_{\chi_1}, \alpha_D = 0.1$



Thermal IDM, $\Delta = 0.1m_{\chi_1}, m_A = 10m_{\chi_1}, \alpha_D = 0.5$



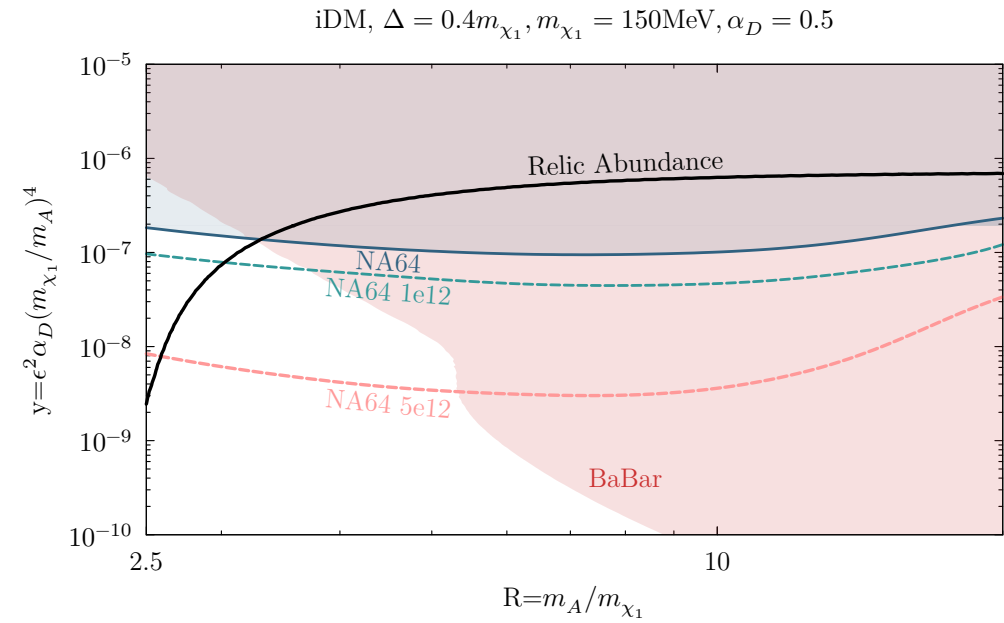
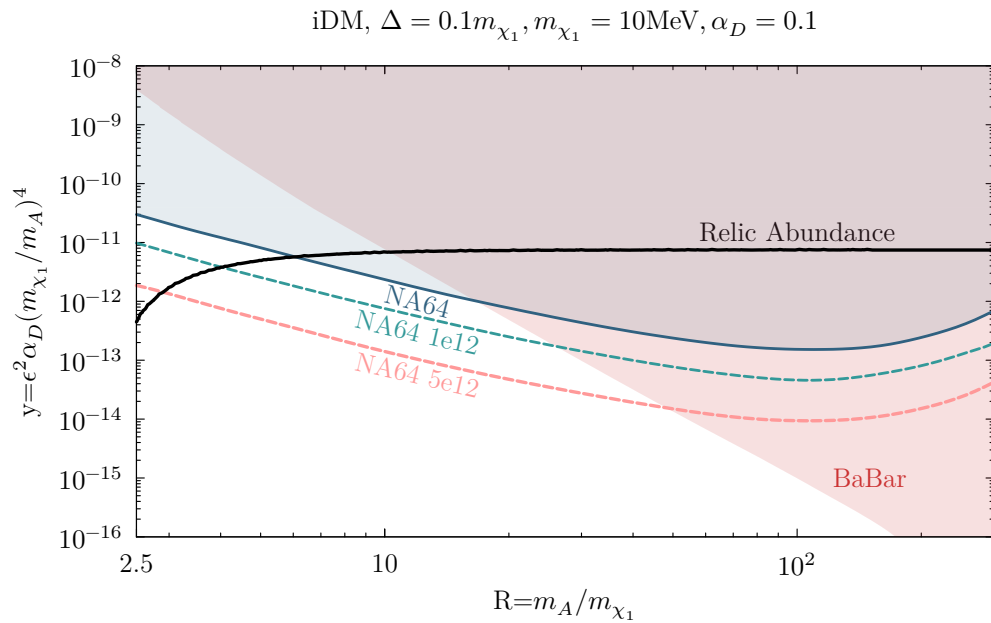
Thermal IDM, $\Delta = 0.4m_{\chi_1}, m_A = 3m_{\chi_1}, \alpha_D = 0.5$



Projections in $m_{\chi_1} - y$ plane:

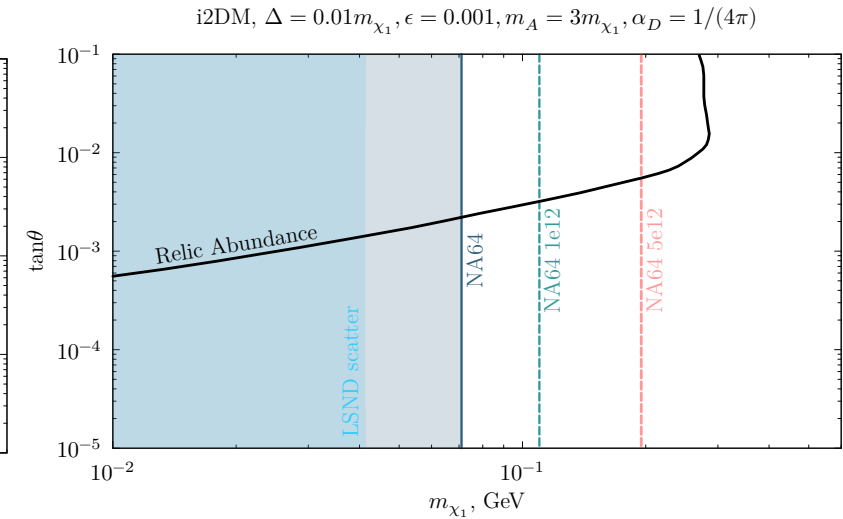
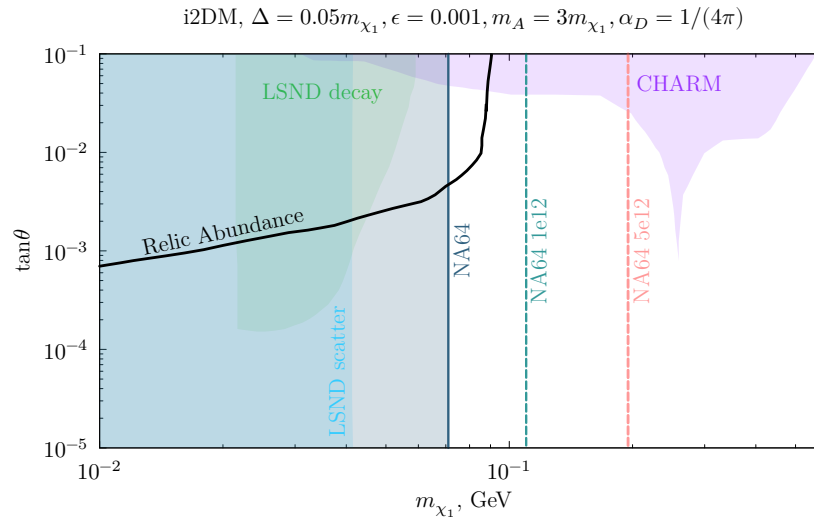
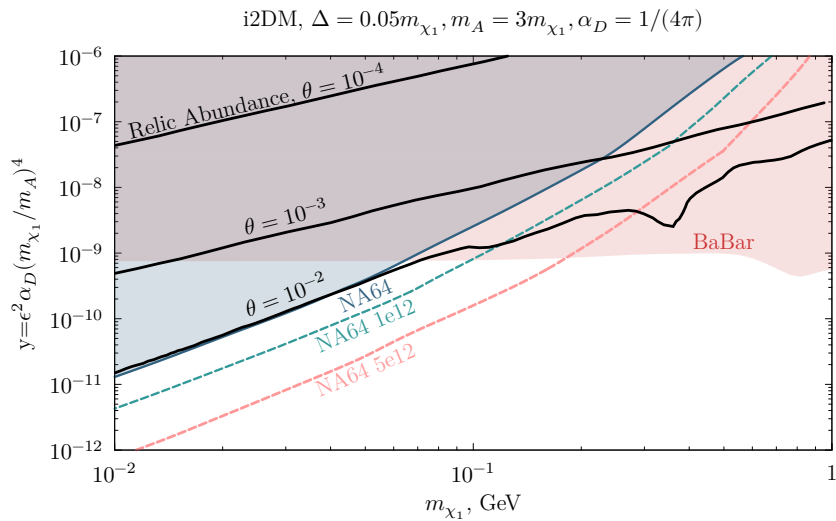
- With 10^{12} EOT: the relic target for $\Delta = 0.4m_{\chi_1}, m_A = 3m_{\chi_1}, \alpha_D = 0.5$ can be further explored
- With $5 \cdot 10^{12}$ EOT: large coverage of the relic targets for different parametrizations

PARAMETER SPACE R vs y – IDM



- Interplay between the experimental sensitivities and the DM relic density as a function of the $R = m_{A'}/m_{\chi_1}$ is often neglected
 - For BP1 (left) the range $R \sim 2.5 - 6$ of the relic line remains unprobed by current searches
 - For BP2 (right) a smaller range within $R \sim 2.5 - 3.3$ is still untested
- With $5 \cdot 10^{12}$ EOT the NA64 sensitivity extends below the standard $R = 3$ point

THERMAL RELIC TARGET – i2DM



Small mass splitting $\rightarrow \chi_2$ is long-lived \rightarrow invisible bounds & reduced sensitivity in displaced vertex searches

$m_{\chi_1} - y$ plane:

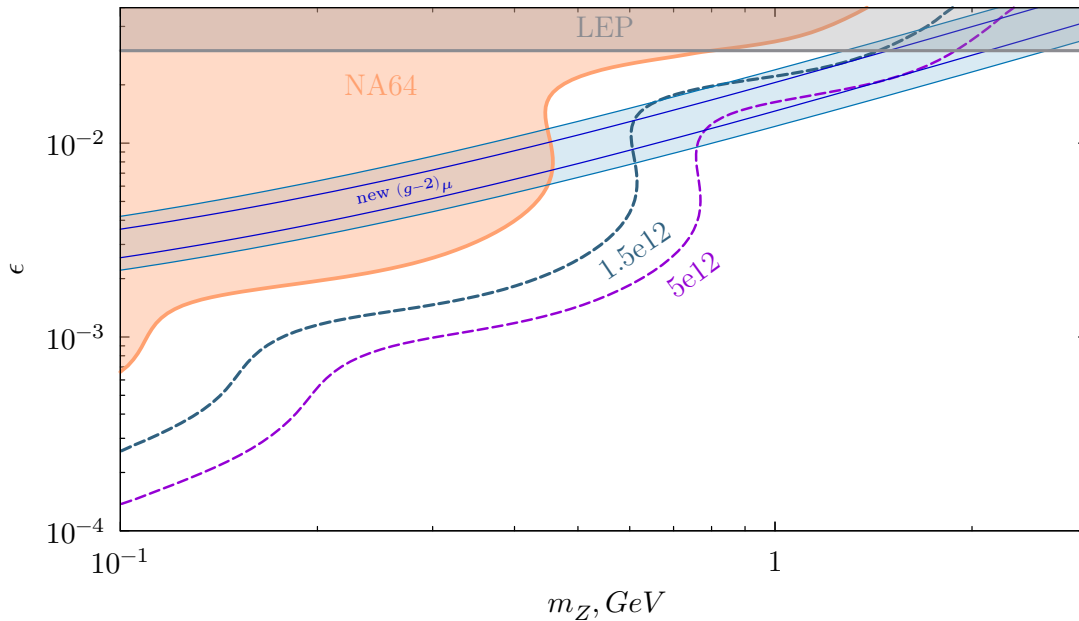
- NA64 bound matches closely the DM relic curve for $\theta = 10^{-2}$ in range $m_{\chi_1} \sim 10 - 50$ MeV
- With 10^{12} EOT: the relic targets for $\theta < 10^{-2}$ can be fully explored

$m_{\chi_1} - \tan \theta$ plane:

- No constraints from BaBar for $\epsilon < 10^{-3}$
- NA64 can set new limits on the minimum allowed DM candidate mass
- With 10^{12} EOT area below $m_{\chi_1} < 110$ MeV can be tested while $5 \cdot 10^{12}$ EOT would increase this value to $m_{\chi_1} < 195$ MeV

SENSITIVITY TO HNL MODEL TARGETING $(g - 2)_\mu$

3HNL, $\alpha_D = 0.75, \Delta_{21} = 0.85, \Delta_{32} = 0.77, m_Z = 6.67m_{N_1}$



Heavy neutral leptons HNL

Ballett et al.
PRD 101, 115025 (2020)
Abdullahi et al.
PLB 820 (2021) 136531
Abdullahi et al.
arXiv:2302.05410

- Motivations:
 - $(g - 2)_\mu$
 - ν mass problem
 - other low E experimental anomalies

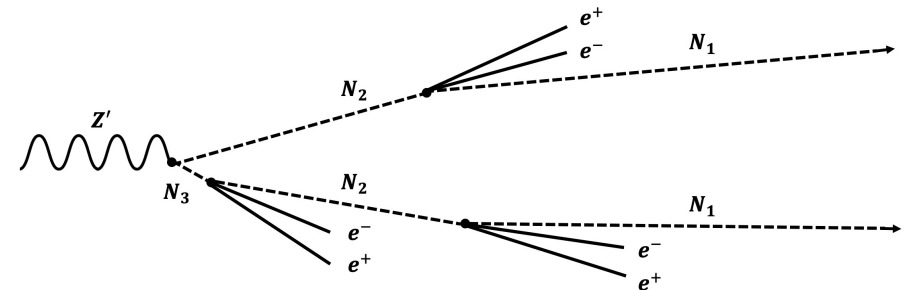
- Benchmark model:

$$\alpha_D = 0.75$$

$$\Delta_{21} = 0.85m_{N_1}, \Delta_{32} = 0.77m_{N_2}$$

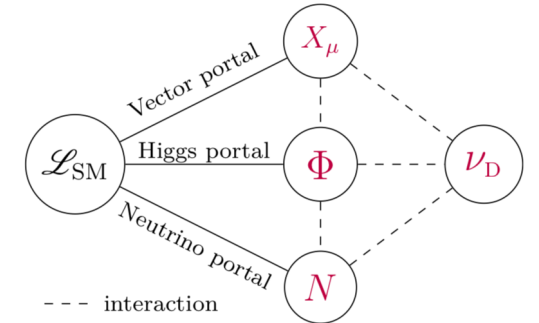
$$m_{Z'}/m_{N_1} = 6.67$$

$$|V_{12}|^2 = 0.01, |V_{23}|^2 = 0.99$$



HNL MODEL

- Exploits a 3 portal connection: vector portal, Higgs portal, neutrino portal



- Based on addition of $U(1)_D$ symmetry but with a richer DS: dark boson A' , dark scalar ϕ , dark neutrino ν_D (charged under $U(1)_D$) and sterile neutrino ν_N (neutral w.r.t. all symmetries)

→ After SSB and mass matrix diagonalization two types of mass ES: ν (SM neutrino) and N (HNL)

$$\mathcal{L}_{HNL} = \mathcal{L}_{SM} + \mathcal{L}'_A + \mathcal{L}_{kin.mix} + \underbrace{(D_\mu \Phi)^\dagger (D^\mu \Phi) - V(\Phi)}_{\mathcal{L}_\Phi} - \underbrace{\lambda_{\Phi H} |H|^2 |\Phi|^2}_{\mathcal{L}_{H-\Phi mix}} + \underbrace{\overline{\nu_D} i \gamma^\mu D_\mu \nu_D}_{\mathcal{L}_{\nu_D}} + \underbrace{\overline{\nu_N} i \gamma^\mu \partial_\mu \nu_N - \left(\frac{\mu'}{2} \overline{\nu_N} \nu_N^c + h.c. \right)}_{\mathcal{L}_{\nu_N}} - \left[\underbrace{y_\nu^\alpha \bar{L}_\alpha \tilde{H} \nu_N^c + y_{\nu_N} \overline{\nu_N} \nu_D^c \Phi + h.c.}_{\mathcal{L}_{\nu-mix}} \right]$$

$$\Gamma(Z' \rightarrow N_i N_j) = |V_{ij}|^2 \frac{g_D^2 m_{Z'}}{12\pi} \left(1 + \frac{\Delta r}{2} \right) (1 - R)^{3/2} \sqrt{1 - \Delta r}$$

$$R = (m_i + m_j)^2 / m_{Z'}^2, \quad \Delta r = (m_i - m_j)^2 / m_{Z'}^2$$

$$\Gamma(N_l \rightarrow N_m e^+ e^-) \simeq |V_{lm}|^2 F(x_{ml}) \frac{(e g_D \epsilon)^2}{384 \pi^3} \frac{m_l^5}{m_{Z'}^4} \quad x_{ml} = \frac{m_m}{m_l}$$

$$F(x) = 1 + 2x - 8x^2 + 18x^3 - 18x^3 + 8x^6 - 2x^7 - x^8 + 24x^3(1 - x + x^2) \ln x.$$